THE JOURNAL OF PHYSICAL CHEMISTRY A
A JOURNAL OF THE AMERICAN CHEMICAL SOCIETY

pubs.acs.org/JPCA

Featured Article

Cold Ion−Molecule Reactions in the Extreme Environment of a Coulomb Crystal

O. A. Krohn and H. J. Lewandowski*

Cite This: J. Phys. Chem. A 2024, 128, 1737−1752

Read Online

ACCESS | Metrics & More | Article Recommendations

ABSTRACT: Coulomb crystals provide a unique environment in which to study ion-neutral gas-phase reactions. In these cold, trapped ensembles, we are able to study the kinetics and dynamics of small molecular systems. These measurements have connections to chemistry in the Interstellar Medium (ISM) and planetary atmospheres. This Feature Article will describe recent work in our laboratory that uses Coulomb crystals to study translationally cold, ion-neutral reactions. We provide a description of how the various affordances of our experimental system allow for detailed studies of the reaction mechanisms and the corresponding products. In particular, we will describe quantum-state resolved reactions, isomer-dependent reactions, and reactions with a rarely studied, astrophysically relevant ion, CCl^+.

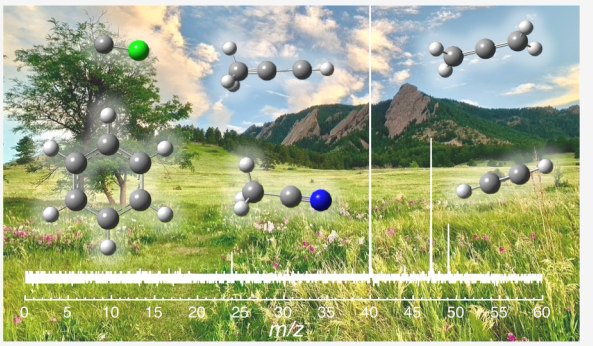

INTRODUCTION

Recent developments in atomic and molecular physics have rapidly expanded the tools available to manipulate and detect molecules. This has presented excellent opportunities to probe the underlying mechanisms of chemical reactions and to apply the knowledge gained to relevant contexts. Ion-neutral, gas-phase chemical reactions are a particularly interesting class of reactions to study; they can be used to understand the fundamental reaction mechanisms in charged systems as well as contribute to the understanding of important chemical environments, such as the Interstellar Medium (ISM).

Historically, understanding the astrophysical environment has inspired substantial ion-neutral reaction research, from laboratory measurements to astronomical observations to computational modeling of this complex space. The complexity and diversity of the chemical composition of the ISM poses a scientific challenge, with at least two hundred unique molecules that have been found in the ISM.[1−5] Modeling the numerous, interconnected reactions that contribute to the current composition of these regions of space is a complicated task, and requires extensive knowledge of the identity, density, and reaction rates of the molecular constituents of the ISM at the relevant temperatures.[6−9] Among the pertinent classes of reactions, ion-neutral interactions play an important role. Ion-neutral reactions often have low or no reaction barriers and are therefore associated with fast reaction rates ($\geq 10^{-11}$ cm^3 s^{-1}). This high reactivity, together with many detected ions and established ionization sources in space, suggests ion-neutral reactions play an important role on determining the present composition of the ISM.[10−12]

The significance of ion-neutral reactions has motivated substantial theoretical efforts.[13] Capture models have been largely successful in predicting the kinetic trends of ion-neutral reactions. These models assume an ion-neutral reaction is dominated by long-range forces and predict rates by estimating the likelihood that a pair of reactants form an adduct. Langevin's reaction rate theory is particularly famous, as it predicts a temperature-independent reaction rate between ions and neutrals that is determined by the neutral molecule's polarizability.[14] Work from Su, Bowers, Chesnavich, and others extended this theory to reflect that long-range effects, particularly the neutral-molecule dipole moment, enhance the likelihood of capture. This leads to an ion-neutral reaction rate with temperature dependence for many systems.[15,16] Similar approaches have been taken in assessing reactions from a quantum-mechanical perspective, especially including effects of the neutral-molecule rotation. This has been particularly necessary, as pioneering tools have enabled reactions at progressively lower energies. Examples of such theory include adiabatic capture centrifugal sudden approximation (ACCSA)[17] and statistical adiabatic channel model (SACM).[18] Such theoretical advances have contributed to our ability to predict the reaction kinetics. These kinetic

Received: November 15, 2023
Revised: January 23, 2024
Accepted: January 25, 2024
Published: February 15, 2024

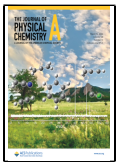

https://doi.org/10.1021/acs.jpca.3c07546
J. Phys. Chem. A 2024, 128, 1737−1752

theories of ion-neutral reactions aid tremendously in ISM modeling, but they are strongest when used in conjunction with experimental investigations.[7]

The collaborative relationship of theory and experiment is perhaps even more evident in foundational explorations of the reaction dynamics. Product branching and reaction mechanisms can elucidate fundamental principles and parameters involved in reaction dynamics.[19,20] To probe these underlying mechanisms, experiments with extensive control of reactant properties and the detection of product characteristics can be very beneficial. One notable frontier for such investigations is the boundary between reactions that can be treated as classical or quantum mechanical.[21−23] As such, a recent direction of the field has been to study this dichotomy of regimes by controlling and reducing the collision energy, while another focus has been to study chemical reactivity across isomers, conformers, and isotopologues. These avenues of inquiry require fine control over the reactants, detection of the products, and extensive theoretical work to understand and analyze the underlying mechanisms.

The experimental realization of ion-neutral reactions has been achieved with many types of experimental setups, each with different advantages and limitations.[21−23] A few historically prominent experimental apparatuses include: selected ion-flow tubes;[24−26] uniform supersonic flows (CRESU);[27,28] crossed-beam methods paired with velocity-mapped imaging;[29,30] and Rydberg−Stark deceleration combined with merged beam methods;[31−33] as well as trap-based methods.[34−36] Some groups, including ours, utilize radio-frequency (RF) traps to study ion-neutral chemical dynamics with Coulomb crystals. The term "Coulomb crystal" refers to the 3D order that can be achieved by ensembles of cold, trapped ions. Such an environment allows us to have precise control over the interactions and to elucidate a new level of understanding of ion−molecule reactions.

This Feature Article will discuss our own work with cold, gas-phase ion-neutral chemical reactions in the environment of Coulomb crystals. We provide a brief overview of our experimental apparatus, highlighting specific features that enable investigations of chemical dynamics. In particular, we discuss Doppler-laser cooling and the opportunities it provides for quantum-state resolved reactions, describe our high-resolution time-of-flight mass spectrometer and the isotopologue tagging it enables, and present the use of selective RF excitations and how we utilized them to trap a unique reactant ion that is difficult to isolate and critical to study.

■ COULOMB CRYSTALS FOR CHEMISTRY

Before discussing our own work with cold, ion-neutral chemical reactions, we provide a brief overview of a selection of previous studies of reactions in Coulomb crystals. While this discussion is not exhaustive and is not intended as a review, it is important to illustrate the diversity and versatility of this experimental design and highlight the excellent progress that has been achieved by the field. The formation of Coulomb crystals relies on laser cooling of an atomic species. Alkaline earth metal ions are a natural choice for laser cooling as there are relatively simple cooling schemes and readily available lasers for these atoms. Doppler laser cooling can cool such ions to mK temperatures; cotrapped ions that are not directly laser cooled can also reach sub-Kelvin translational temperatures due to the Coulomb forces between ions in the trap.[37−40] Cold, trapped ions at these temperatures form an ordered crystallike, ellipsoidal structure. An image of a cross-sectional slice of an ellipsoidal crystal is shown in Figure 1, where individual ion sites can be viewed by the fluorescence emitted from the ions. Note that sympathetic cooling allows for only translation cooling of cotrapped molecules, not cooling of internal degrees-of-freedom. Electronic and vibrational states can be allowed to relax in a typical reaction experiment as they are relatively short-lived compared to the lifetime of ions in the trap. However, rotational states are often pumped by blackbody radiation of the room-temperature UHV chamber walls. When these crystals are formed in dynamic RF traps and ultra high vacuum (UHV) environments, ion ensembles can be stable for hours and provide abundant opportunities to manipulate and probe the system, including studying ion-neutral, gas-phase reactions.[41−45]

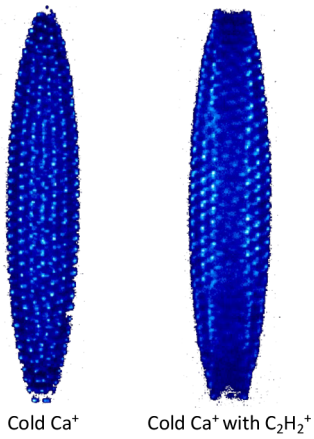

Figure 1. False-color images of the fluorescence from two Coulomb crystals, one of pure laser-cooled calcium ions (left), and the other with cotrapped, sympathetically cooled acetylene ions (right). The acetylene ions are trapped near the center and, because they do not fluoresce, are seen as a dark core in the crystal. These images are taken by an intensified CCD camera using a microscope objective positioned above the RF trap.

In one such set of studies of crystals, reactions have demonstrated isotope-specific dynamics. An early example of such an investigation is that of laser-cooled Mg^+ reacted with HD, demonstrating a branching ratio of MgD^+ to MgH^+ of 5 to 1.[46] A more recent paper reported an inverse kinetic isotope effect (in which reactions with the deuterated neutral are significantly faster than those with the hydrogenated neutral) for ammonia reacting with rare gas ions Xe^+, Kr^+, and Ar^+.[47,48] A small inverse KIE was also observed in a merged-beam reaction of Rydberg−Stark decelerated He^+ with both isotopologues of ammonia. This study demonstrated a faster reaction of $He^+ + ND_3$ over $He^+ + NH_3$.[49] Such isotope effects are unexplained by classical kinetic reaction rate theories, which predict slightly slower reactions in the deuterated case. These inverse cases may be particularly relevant to understanding the greater presence of deuterated molecules in the ISM than is expected from the relative abundances of hydrogen and deuterium (a phenomenon referred to as deuterium fractionation).[50]

Studies have also demonstrated that chemical dynamics can be fundamentally influenced by the structural and spatial isomers of the reaction participants. One example from our group is the reaction of $C_2H_2^+ + C_3H_4$, which is dominated by long-range charge transfer for the allene isomer of C_3H_4, but is

https://doi.org/10.1021/acs.jpca.3c07546
J. Phys. Chem. A 2024, 128, 1737−1752

influenced by short-range effects for propyne.[51,52] This example will be discussed in depth later in this article. Another example of isomer-resolved chemistry includes the work of Yang et. al, in which trapped C^+ was reacted with water from a cryogenic buffer-gas beam to form HCO^+ and HOC^+ at cold (~20 K) temperatures.[53] The branching ratio of these two product isomers was determined by a second ("titration") reaction with neutral nitrogen gas, as HOC^+ reacts to form N_2H^+, while HCO^+ does not. This reaction demonstrated an important formation mechanism for HOC^+ in an interstellar medium.

Another class of isomers with chemical ramifications are stereoisomers, which have the same molecular connectivity but are distinguished by different spatial arrangement. While traditionally difficult to isolate, recent work has succeeded in using highly inhomogeneous electric fields to differentially deflect the stereoisomers of two molecules, dibromobutadiene and 3-aminophenol, by their dipole moments, such that reaction rates can be measured as a function of the relative population of the two isomers.[54,55] Recent studies have demonstrated an enhanced reaction rate in the isomer with the higher dipole moment; theoretical modeling of the reaction attributed this effect to stronger suppression of the centrifugal barrier and, thus, greater likelihood of capture for the isomer with the larger dipole moment. Trapping and sympathetic cooling of individual conformers in a Coulomb crystal has also been recently achieved.[56] Studies of reaction dynamics with control over isomeric and isotopic variables in Coulomb crystal environments have proven productive and continue to be an avenue of interest.

Efforts to tune the energy of the neutral reactant in Coulomb crystal studies have been fruitful, as well. With the use of quadrupole guides, several molecules with large Stark shifts have been filtered to lower velocities. This "Stark filtering" has been demonstrated for many molecules, the most common examples of which are CH_3F, ND_3 and CH_3CN.[57−59] A recent application of this method was demonstrated by Okada et al. in a reaction between cold, trapped Ne^+ and velocity-filtered CH_3CN. The reaction demonstrated an increasing reaction rate with decreasing collision energy over $20\ \mathrm{K} \geq T \geq 5\ \mathrm{K}$ (where $T = E/k_B$, E is energy, k_B is Boltzmann's constant).[60]

Some methods have further exhibited control over the quantum state of the neutral reactant with the combination of an ion trap with a magneto-optical trap (MOT).[61] One such MOT-ion hybrid trap demonstrated a "blockading effect" whereby the radiative lifetime of an excited state of a reactant is comparable to the reaction complex lifetime and influences the reaction dynamics. Puri et al. studied the $Ca + BaCl^+$ reaction over $15\ \mathrm{K} \geq T \geq 0.2\ \mathrm{K}$ and demonstrated the suppression of the reaction rate at low energies due to the short lifetime of the Ca excited state.[62] Likewise, the quantum state of the ion can also be manipulated for reactivity studies by utilizing the laser-cooling cycle required to form Coulomb crystals.[57,63−65] This method will be discussed in more detail later in this article with an emphasis on our own investigations of the electronic-state-dependent reaction of Ca^+ with NO.

A LIT-TOFMS FOR ISM AND FUNDAMENTAL CHEMISTRY INVESTIGATIONS

A rendering of our experimental apparatus used for gas-phase reactions of cold, trapped ions with neutral molecules is shown in Figure 2. This system is under ultra high vacuum (UHV),

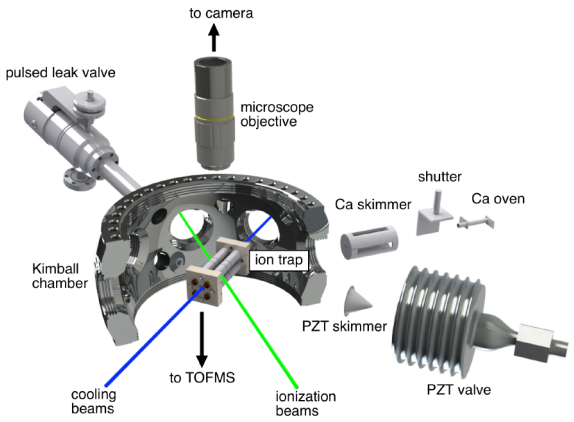

Figure 2. Schematic rendering of the LIT-TOFMS used for ion-neutral reactions. Calcium ions are loaded from a effusive calcium oven source crossed with a tripled Nd:YAG at 355 nm. Reactant ions are loaded by photoionization of a skimmed molecular beam by the output of a frequency-doubled pulsed dye laser. Ions can be observed by fluorescence of the laser-cooled calcium and counted with time-of-flight mass spectrometry. The microscope objective and pulsed leak valve are the only parts in the diagram outside of the UHV vacuum chamber. Adapted with permission from Schmid et al.[51] Copyright 2020 PCCP Owner Societies.

with pressures on the order of $\sim 10^{-10}$ Torr. At the center of this experiment is a linear Paul ion trap, which dynamically traps ions with a trapping frequency of 3.555 MHz and a typical magnitude of 300 Vpp. As previously mentioned, ensembles of laser-cooled calcium ions in this environment achieve low temperatures and form Coulomb crystals. While the oscillating RF fields cause "micromotion heating" to energies equivalent to $\lesssim$10 K, the average motion is very small, resulting in "secular temperatures" in the millikelvin regime. Reactant ions other than calcium can also be cotrapped and sympathetically cooled within this Coulomb crystal environment, such that reactions with any trapped ion species can occur at translationally cold temperatures.

Several of the components labeled in Figure 2 are used for loading ions into the trap. A calcium oven serves as an effusive source of calcium. During loading, a shutter is opened to allow calcium through a skimmer to the trap center, where the calcium crosses paths with the ionization laser (tripled Nd:YAG, 355 nm) in the center of the trap. The trapped Ca^+ ions are cooled by two diode lasers on the Ca^+ cooling 397 nm transition, with a 866 nm laser for repumping from the dark $D_{3/2}$ state.

In some cases, Ca^+ itself serves as the ionic reactant. Other reactions involve noncalcium "dark" ions coloaded into the crystal. These dark ions are loaded by seeding a molecule precursor into a rare gas to produce a cold, skimmed, molecular beam using the piezoelectric valve and skimmer shown in Figure 2. The precursor is multiphoton ionized with ultraviolet (UV) light from a frequency-doubled pulsed dye laser. In some cases, resonant ionization of the precursor leads to relatively pure samples of the reactant ion in the trap. In other cases, the trap contents needed to be filtered or cleaned. Cleaning of the trap is achieved by taking advantage of the secular frequencies that are unique to each m/z ratio of ions in the trap, which can be ejected with dipolar[66] or quadrupolar[67] excitations. Quadrupolar excitations (also called parametric excitation) modulate the depth of the trap at the secular

https://doi.org/10.1021/acs.jpca.3c07546
J. Phys. Chem. A 2024, 128, 1737−1752

frequency of the contaminant ion and are particularly effective at cleaning our trap.

Reactions begin after a cold, clean sample of reactant ions and Ca^+ are loaded, and a Coulomb crystal is formed. The t = 0 start of the reaction is defined by the opening of the leak valve that introduces $\sim 10^{-9}$ Torr of gas through a variable leak valve backed by a three-way valve. This allows for very fast (about a second) opening and closing as well as excellent reproducibility in the gas pressure during each exposure to neutral gas. The gas introduced is usually a ∼5−15% mixture of the reactant gas in an inert gas, usually Ar, He, or N_2. The resulting partial pressures generally require an exposure time on the order of hundreds of seconds for all of the initial ions to react. This is sufficiently slow to clearly differentiate between the primary and secondary products.

Ion trap contents are probed with time-of-flight mass spectrometry (TOF-MS). We choose several time points to destructively measure the m/z of the ions by quickly (in a single RF cycle) quenching the RF and sending a high-voltage pulse to the trap rods. The ions are then accelerated into a flight tube toward a microchannel plate detector (MCP), where the signal magnitude and timing are used to determine the number and m/z of ions, respectively, that were in the trap. By changing the time at which we eject the ions, we can determine the number of ions in various product channels as a function of neutral gas exposure time and delineate the reaction order of products. Our TOF-MS has a resolution of $m/\Delta m \geq 1100$, more than sufficient to resolve masses differing by 1 amu. In addition to high resolution, our TOF-MS detection is quite sensitive such that we can discern single ion counts and quantitatively measure the product ions in all mass channels. Together, these components of the experiment allow for quantitative measurement of the product masses and reaction rates for translationally cold, ion-neutral chemical reactions.

Several experimental studies that have been conducted in this apparatus have required unique features of the experimental apparatus. The remainder of this Feature will focus on three techniques utilized in this experimental apparatus; each of these techniques will be paired with an ion-neutral study that we were able to investigate only using this technique. The next section will discuss the laser cooling of the Ca^+ ions in more detail and describe how this allows quantum-state resolved reactions in our apparatus. Section will discuss high-resolution mass spectrometry in more detail, followed by a discussion of a reaction study that required reactant deuteration and discrimination between neighboring product mass channels to determine the reaction mechanism. Section will describe how we leverage aspects of electrodynamic trapping to selectively clean our trap. This technique allowed us to explore reactions with an ion that has been historically challenging to isolate in pure samples.

DOPPLER COOLING AND QUANTUM-STATE DEPENDENT REACTIONS

Coulomb crystals are typically created by laser cooling ions, while they are contained in a strong electrodynamic trap. Through standard Doppler laser-cooling techniques, ions can be cooled to millikelvin temperatures. At these temperatures, the kinetic energy is low enough that the combination of ion−ion Coulomb forces and the trapping potential result in a pseudocrystalline structure (Figure 1). The laser-cooled ensembles have many advantages for reaction experiments, including operating at low temperatures, visually monitoring the trapped atomic ions, and allowing quantum-state control of atomic ion reactions.

The primary reason for laser-cooling is to reach low temperatures. Direct cooling of the Ca^+ ions and sympathetic cooling of cotrapped "dark ions" enables temperatures below or on the order of ∼10K, even when accounting for micromotion heating of the trap. Depending on the neutral reactant source, the resulting collision energies can be in the cold or ultracold regime. In our experiments with room temperature thermal gas, collision "temperatures"[1] are typically around 100−150 K, depending on the mass of the reactants.

Another advantage of laser-cooled samples is that the atomic ions scatter many photons in the cooling cycle. In addition, even very cold ions are spaced ∼10 μm away, allowing for resolution of their spatial locations. The fluorescence from the crystal can be imagined onto a camera, yielding images such as Figure 1. Here, the crystal has been cooled to a sufficiently low temperature such that each individual ion site can be observed. Note that although a single ion location can be resolved, ions do hop between sites and the overall crystal structure can change as a function of time. These images of the Coulomb crystal can be used in many ways to study reactions. At a basic level, one can qualitatively determine the "temperature" of the crystal by looking at how well the ions are resolved or if the crystal has melted. These simple checks give the researcher feedback as to whether the trapping and cooling are working well.

In addition, the collection of scattered light has historically been used as a source of information about the constituents of the ion trap. An early technique to determine the mass of ions in the trap was to sweep through potential secular frequencies of ions in the trap, measuring the velocity-dependent amount of scattered light.[68,69] More recently, groups have utilized images of the Coulomb crystal to infer population of "dark" reactant and product ions by their deformation of the laser-cooled ion positions, usually aided by comparison to molecular dynamics simulations.[47,58,59,70,70,71] In our own group, we use the image of the initial Ca^+ crystal to normalize the TOF-MS data when studying the reaction of Ca^+ with nitric oxide (NO), which will be discussed in the next subsection.

A final advantage of laser cooling, which will be highlighted in the next section, is the opportunity to manipulate the quantum-state populations of the laser-cooled ions. The steady-state excited-state population of laser-cooled ions in the trap is inherently dependent on the detuning from the resonance of the cooling lasers. The population in each of the electronic states can be manipulated to examine the state dependence of reactions of neutral molecules with laser-cooled ions. This technique has been demonstrated in ion traps with a variety of laser-cooled ionic species.[57,63,70−74] This includes two examples studied within our own group: the quantum-state-resolved study of Ca^+ with O_2[65] and NO.[64] The Ca^+ + NO reaction involved two product states with a discernible dependence of the $P_{1/2}$ state population. The experimental details, results, and chemical relevance of the quantum-state-resolved measurement of Ca^+ + NO will be discussed in the next section.

Quantum-State Controlled Reaction of Ca^+ with the NO Radical. Free radicals and ions have been established as important groups of molecules present in the interstellar medium.[4,5] These molecules are quite reactive, as their

https://doi.org/10.1021/acs.jpca.3c07546
J. Phys. Chem. A 2024, 128, 1737−1752

reactions are usually barrierless at very cold temperatures, and thus their presence influences the chemical composition of many regions of space.[10,75−77] However, experimental measurements of ion-radical reactions are rather rare as both ions and radicals are difficult to create in dense, pure samples. Coulomb crystals are an advantageous environment for such reaction studies, as long interaction times and sensitive detection of products alleviate the disadvantages of low densities. In the case of Ca^+ + NO, we were able to measure products with reaction rates on the order of 10^{-12} cm^3/s, by allowing interaction times that were several minutes in length. This was the first study of an ion-radical reaction with quantum-state control over the electronic state of the ion.

The importance of the excited-state levels of Ca^+ to the reaction Ca^+ + NO can be observed from the energy diagram shown in Figure 3. The electronic states corresponding to our

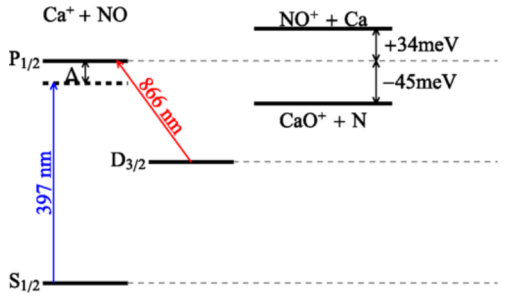

Figure 3. Energy diagram for the reaction of Ca^+ + NO. (left) Relevant energy states of Ca^+, with the cooling laser wavelengths marked on the appropriate energy transitions. (right) The relative product energy for the NO^+ + Ca and CaO^+ + N demonstrated exothermicity for the CaO^+ product and slight endothermicity for the NO^+ product from the Ca^+ $P_{1/2}$ state. (Energies not to scale.) Reprinted from Greenberg, J. et al. *Phys. Rev. A* **2018**, *98*, 32702.[64] Copyright (2018) by the American Physical Society.

laser-cooling scheme are shown on the left. The steady-state fraction of the population excited to the $P_{1/2}$ state can be controlled by adjusting the detuning, Δ, from the $S_{1/2}$−$P_{1/2}$ transition. Ca^+ may react with radical molecule NO to form either NO^+ + Ca or CaO^+ + N, but only from the $P_{1/2}$ excited state. High-level coupled-cluster theory and HEAT thermochemical protocol were utilized to determine the thermochemistry of this reaction.[78] The formation of the CaO^+ product was determined to be exothermic by 45 meV for the reaction from the excited $P_{1/2}$ state. The NO^+ + Ca, on the other hand, was calculated to be endothermic by 34 meV. Note that the reaction of room-temperature NO and cold Ca^+ was $\bar{E}_{coll}/k_BT$ ∼ 180 K or 16 meV. Some fraction of the reactants were able to surmount the energetic barrier to form NO^+.

We studied the reaction-rate dependence on both the NO concentration and the fractional population of Ca^+ in the $P_{1/2}$ state. Because the NO was in excess, this reaction was modeled as a pseudo-first order reaction with a certain fraction of the total Ca^+ ion numbers representing the available ionic reactants. This can be expressed mathematically,

$$\frac{NO^+(t)}{Ca^+(0)} = \frac{k_{NO}}{k_{NO} + k_{CaO}}\left(1 - \exp^{-k_{NO}[NO]f_P t}\right) \quad (1)$$

$$\frac{CaO^+(t)}{Ca^+(0)} = \frac{k_{CaO}}{k_{NO} + k_{CaO}}\left(1 - \exp^{-k_{CaO}[NO]f_P t}\right) \quad (2)$$

where the f_P is the fraction of Ca^+ in the $P_{1/2}$ state, [NO] is the concentration of NO molecules leaked into the chamber, and the number of $NO^+(t)$ and $CaO^+(t)$ product ions at time t are normalized by the number of calcium ions at t = 0, $Ca^+(0)$. This model was used to fit the reaction data and derive the reaction rate constants k_{NO} and k_{CaO}. An example reaction curve is shown in Figure 4. The data points and error bars

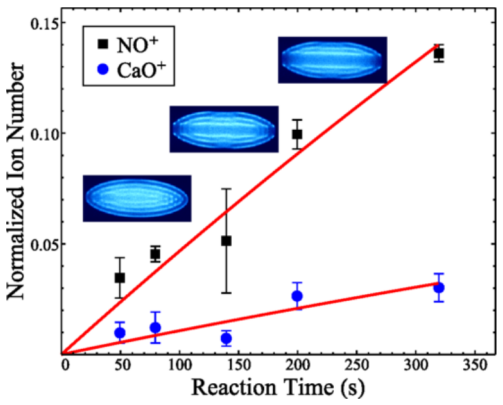

Figure 4. Product NO^+ and CaO^+ normalized ion numbers as a function of time. Example false-color fluorescence images of the Coulomb crystals just before ejecting the ions into the TOF-MS are shown for t = 50, 200, and 320 s. The dark bands in the center and on the outside show trapped ions lighter and heavier than Ca^+, respectively. Reprinted from Greenberg, J. et al. *Phys. Rev. A* **2018**, *98*, 32702.[64] Copyright (2018) by the American Physical Society.

represent the mean and standard error, respectively, for the products NO^+ and CaO^+. The red lines represent best fits of the data according to the pseudo-first-order reaction-rate model described by eqs 1 and 2.

However, in order to derive a reaction rate constant from these fits, we required knowledge of [NO] and f_P. We repeated the measurement over multiple values of [NO] and f_P to determine the overall reaction-rate dependence on the two independent variables. The dependence of f_P on the cooling laser wavelength was derived using optical Bloch equations.[57] The NO concentration was determined by ion gauge readings. These two studies of the reaction rate should be self-consistent in their measurements, assuming there are no systematics present. We found the two independent analyses to be in agreement, as shown in Table 1.

In summary, this quantum-state resolved reaction study demonstrated the reactivity of Ca^+ in the $P_{1/2}$ state with the radical NO. The concentration of NO and the $P_{1/2}$ fractional

Table 1. Rate Constants and Branching Ratios, with Statistical Uncertainties from Two Independent Measurements[a]

	NO concentration	$P_{1/2}$ fraction
k_{NO} (cm^3/s)	2.3(2)× 10^{-11}	2.7(3) × 10^{-11}
k_{CaO} (cm^3/s)	4.4(7)× 10^{-12}	7(2) × 10^{-12}
BR_{NO}	0.8(2)	0.8(1)
BR_{CaO}	0.21(5)	0.16(3)

[a]One measured the rate dependence on the NO concentration; the other rate measurement was fit from varying the fraction of Ca^+ in the electronic $P_{1/2}$ state. Uncertainties represent statistical uncertainties. Reprinted from Greenberg, J. et al. *Phys. Rev. A* **2018**, *98*, 32702.[64] Copyright (2018) by the American Physical Society.

https://doi.org/10.1021/acs.jpca.3c07546
J. Phys. Chem. A 2024, 128, 1737−1752

population were independently manipulated to determine the reaction rate constants and branching ratios. The measurements agreed within the statistical uncertainty, demonstrating that the electronic states were carefully and effectively controlled to manipulate the reaction rate. This reaction not only demonstrated a quantum-state controlled reaction but also was the first reported example of such control in an ion-radical chemical reaction.

TOF-MS AND ISOMER-SPECIFIC CHEMISTRY

The second technique utilized in our experimental apparatus that we highlight in this Feature is time-of-flight mass spectrometry, which is a relatively new addition to chemical reaction studies in Coulomb crystals. (It is, however, not new to ion traps, where it has been extensively used for ion spectroscopy.[79−81]) As previously mentioned, the m/z of ions in a trap was historically determined using the scattered light from trapped, laser-cooled ions. This can be achieved by observing scattered fluorescence while an additional excitation is swept over the secular frequencies of applicable ions masses.[68,69] This method can achieve good resolution with careful implementation in two-ion systems; however, this technique is poorly suited for quantitative measurements of ions in three-dimensional Coulomb crystals, where Coulomb coupling impacts both the position and widths of the motional resonances, complicating the accuracy and hindering the precision of this method.[82] For this reason, groups that study chemical reactions in Coulomb crystals now typically detect reaction products with image analysis of the Coulomb crystal or with time-of-flight mass spectrometry.

Recent advances in the efficiency of molecular dynamics simulations have enabled groups to simulate images of the Coulomb crystal to infer population of "dark" reactant and product ions by their deformation of the laser-cooled ion positions.[47,48,58,59,70,71] This can be a powerful technique, particularly as images of the crystal can be compared within the same reaction sequence, eliminating the uncertainty from variations in ion loading numbers. This technique has only been demonstrated for reactions with laser-cooled ions,[47,58,59,71] or with single-product reaction mechanisms, such as charge-exchange or hydrogen abstraction processes.[48,58,59,70] While this method has the benefit of being nondestructive, it is not suitable for all reactions, especially those with multiple product ion channels. Also, achieving accuracy to single ion numbers is very difficult.

A more flexible and high-resolution approach for ion detection is time-of-flight mass spectrometry (TOF-MS). Most groups that conduct reaction studies in Coulomb crystals have developed and coupled TOF-MS systems to their linear ion trap.[83−85] Our own linear ion trap is coupled to a TOF-MS that has a mass resolution of $m/\Delta m > 1100$.[44] This is more than sufficient to resolve neighboring masses for our typical range of $m/z < 100$. With high-resolution detection across this full span of masses, we observe both the growth of product ions, as well as the decay of reactant ions. From these simultaneous measurements, we are able to determine conservation of total number of ions throughout the reaction, which is necessary to accurately measure branching ratios. In contrast to imaging methods, mass spectrometry measurements are destructive in nature. As such, an investigation of a full reaction requires a mass spectra to be measured multiple times at several time points.

Naturally, the detection of product m/z ratios with high precision has been important for all of our reaction studies; however, the high precision within our system has been particularly important for studies in which mass shifts from deuterated reactants elucidate the product identity or reaction mechanism. This has been exemplified by two reactions investigated by our group, reactions of the acetylene cation with acetonitrile,[86] and with isomers of C_3H_4.[51,52] The details of the experimental and computational exploration of the latter are the topic of the next section.

Isomer-Specific Dynamics in the Reaction of $C_2H_2^+$ + C_3H_4. The $C_2H_2^+ + C_3H_4$ reaction is relevant to astrochemistry for a few reasons. Hydrocarbons are abundant throughout the regions of space. In particular, acetylene (C_2H_2) has been a molecule of interest since its early discovery in the ISM in 1989.[87−91] Reactions between acetylene and other hydrocarbons are key to understanding carbon chain growth.[10,92,93] This interest in progressive addition to hydrocarbons extends to allene and propyne as well.[89,93] The opportunity to compare reactions with the two isomers, their products, and the impacts of deuteration is beneficial for modeling and understanding this class of hydrocarbon reactivity.

In addition to its astrochemical importance, the reaction of acetylene cation with C_3H_4 demonstrated isomer-specific dynamics that were discerned with the use of high-resolution mass spectrometry. We reacted acetylene ions with two C_3H_4 isomers: propyne (also called methyl acetylene, HC_3H_3) and allene (also called propadiene, $H_2C_3H_2$.) The isomers demonstrated two inherently different reaction mechanisms and product branching ratios.[51,52] With isotope substitution, there were 12 different reactions that were investigated, which included two isotopologues of acetylene ($C_2H_2^+$, $C_2D_2^+$), two isotopologues of allene ($H_2C_3H_2$, $D_2C_3D_2$), and four isotopologues of propyne (HC_3H_3, DC_3H_3, HC_3D_3, DC_3D_3) as shown in Figure 5. Comparison of product isotopologues

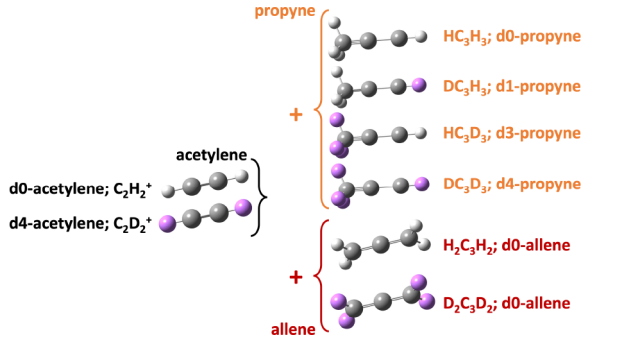

Figure 5. Diagram demonstrating the isomers and isotopologues of the reactants we studied. On the left, the two isotopologues of acetylene ions are depicted, which were reacted with four isotopologues of propyne and two isotopologues of allene.

across these reactions was instrumental in identifying the contrasting reaction mechanisms for allene and propyne. The ability to effectively interpret the results of such isotopologue substitution was dependent on the quality and fidelity of our mass spectrometry.

The experimental results will be discussed first, followed by the calculated potential energy surface. Both the experimental and theoretical results revealed consistent evidence of a significantly different reaction mechanism for the reaction of

https://doi.org/10.1021/acs.jpca.3c07546
J. Phys. Chem. A 2024, 128, 1737−1752

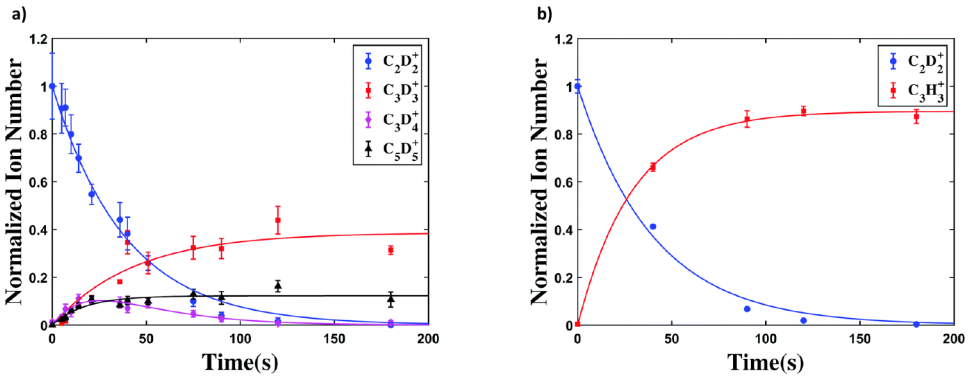

Figure 6. Normalized relative populations of m/z as measured by mass spectrometry, plotted with respect to the time exposed to the neutral reactant. (a) Reaction $C_2D_2^+ + DC_3D_3$ produces multiple primary products: $C_3D_3^+$, $C_3D_4^+$, and $C_5D_5^+$. Note that $C_3D_4^+$ further reacts with DC_3D_3 to form the second-order products $C_6H_5^+$ and $C_6H_7^+$, which are not shown in this figure. (b) Reaction $C_2D_2^+ + H_2C_3H_2$. Most of the products are $C_3H_3^+$. While a very small amount of $C_3H_4^+$ is also produced, it undergoes a secondary reaction fairly quickly and does not accumulate in significant numbers. Adapted with permission from Schmid et al.[51] Copyright 2020 PCCP Owner Societies.

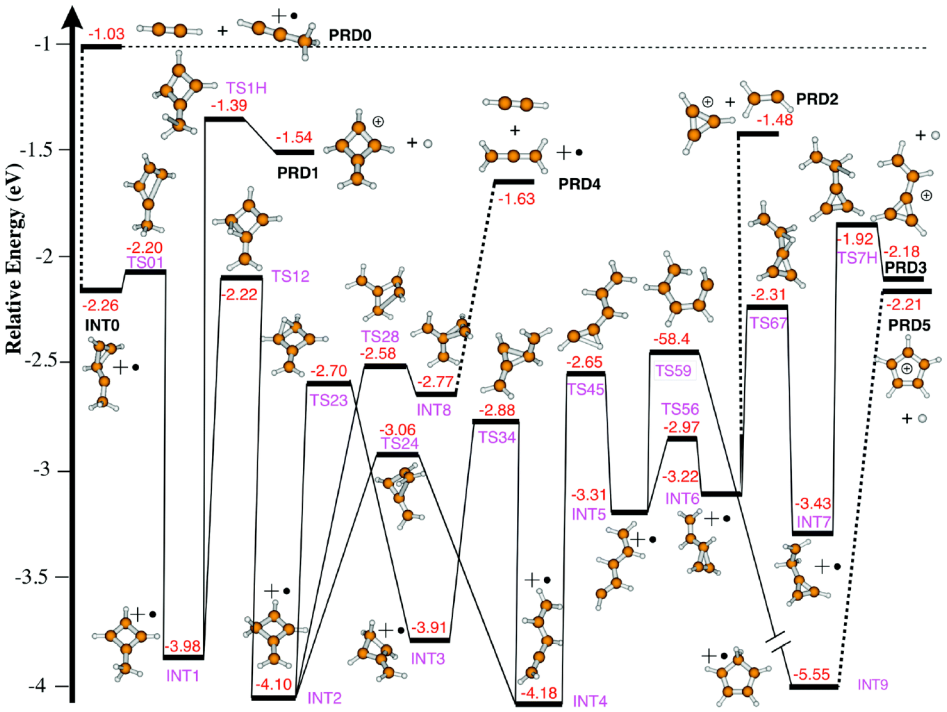

Figure 7. Potential energy surface bridging the close-range charge exchange complex of acetylene cation and propyne to experimentally observed products. "INT" refers to intermediate states, "TS" to transition states, and "PRD" to products. All energies are shown relative to the original acetylene cation and propyne energy in eV. However, PRD0 (top left) is already after the initial charge exchange between $C_2H_2^+ + HC_3H_3$, at ∼1 eV exothermicity. Dashed lines between stationary points indicate that reactions occur via loose transition states. Adapted with permission from Schmid et al.[51] Copyright 2020 PCCP Owner Societies.

acetylene with propyne and allene. Potential causes for this difference will be discussed last.

Normalized ion numbers as a function of time that the ions were exposed to the neutral reactant gas are shown in Figure 6. The diversity of the reaction products is distinctly different for the two reactions. In the case of acetylene cations reacting with propyne, the primary products include three channels: $C_3D_3^+$, $C_3D_4^+$, $C_5D_5^+$; in contrast, acetylene cations reactions with allene produced almost solely $C_3H_3^+$ (with a few percent yield of $C_3H_4^+$). The presence of $C_5D_5^+$ is notable, as it is a product that requires a reaction complex to form. In studying all the isotopologue combinations, a greater contrast between the dynamics of the two reactions becomes evident. For the propyne reaction, the product mass channels split in the case of mixed reactant isotopologues (where reactants contained both hydrogen and deuterium,) indicating "scrambling" of hydrogen and deuterium in a reaction complex. This scrambling of product isotopologues is consistent with a reaction mechanism wherein short-range charge transfer is followed by bond formation. Such a mechanism is also supported by the observation of the $C_5D_5^+$ product, which requires reaction complex formation to form. This overall trend in the propyne reaction contrasted with the case of allene, where no observed scrambling of hydrogen and deuterium was observed. Instead the reaction of d0-allene or d4-allene with acetylene formed $C_3H_3^+$ or $C_3D_3^+$, respectively, regardless of the acetylene

https://doi.org/10.1021/acs.jpca.3c07546
J. Phys. Chem. A 2024, 128, 1737−1752

isotopologue. This precluded a reaction mechanism whereby the hydrogen and deuterium atoms could exchange, inferring a long-range charge transfer process that led to no complex formation.

The potential energy surfaces (PESs) for the two reactions are also quite different. Details regarding the theoretical methods can be found in the original paper, as well as previous work by Nguyen and Stanton.[51,52,94] The potential energy surface for the acetylene cation and propyne reaction will be discussed first, followed by the surface for the acetylene cation and allene reaction.

The PES for $C_2H_2^+$ + d0-propyne is shown in Figure 7. The first state after the charge transfer is PRD0, which is already ∼1 eV exothermic with respect to the original reactants. PRD0 is a possible product that is detected with a small branching ratio. The majority of the $C_3H_4^+$ and C_2H_2 collisions form a $C_5H_7^+$ complex, (INT0.) From INT0 several exothermic pathways to products are possible, and all of these products are observed in the experiment. The predicted products are $C_3H_4^+$ (PRD0, PRD4), $C_5H_5^+$ (PRD1, PRD3, PRD5), and $C_3H_3^+$ (PRD2), agreeing with the experimental observations. Overall, the PES supports the description of the acetylene cation and propyne reaction as being dominated by charge transfer followed by the formation of an association complex to produce the experimentally measured product ions.

As with the experimental data, the PES for the acetylene cation and allene reaction shown in Figure 8 also contrasts

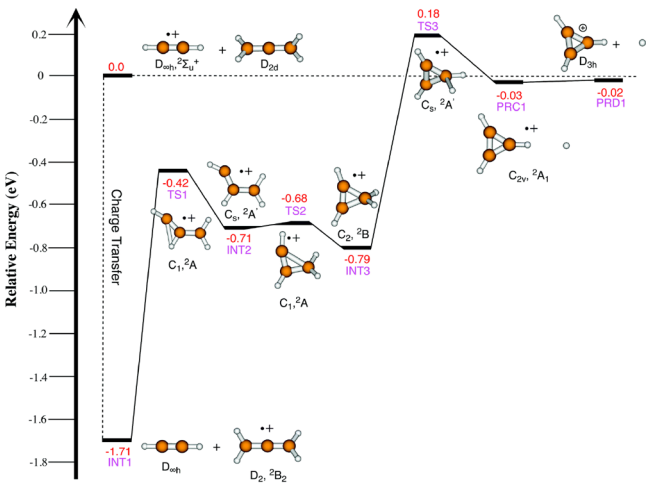

Figure 8. Potential energy surface showing a pathway from d0-allene and d2-acetylene reactants to the observed $C_3H_3^+$ product. "INT" refers to intermediate states, "TS" to transition states, and "PRD" to products. The reaction proceeds via quantum tunneling through TS3 to form a nearly isoenergetic product. The + between molecules for the initial reactants and INT1 denotes that the energies were calculated with the two molecules at infinite separation. Adapted with permission from Schmid et al.[51] Copyright 2020 PCCP Owner Societies.

with the propyne reaction. The first notable difference from the propyne reaction is seen in the first intermediate state, INT1. The charge exchange is exothermic by −1.71 eV and results in Jahn−Teller distortion of the molecule to shift the symmetry from D_{2d} to D_2. This distortion has ramifications for the reaction mechanism, as it suggests that the energy gained from the charge transfer is more likely to be localized in the allene cation than in the propyne case, as propyne does not undergo a significant structural change when ionized. This distortion in the allene cation discourages bond formation. This also enables the available energy to be used in isomerization. This is indeed the pathway demonstrated theoretically: the PES shows unimolecular isomerization of the allene ion through two submerged barriers (TS1 and TS3) and a slightly endothermic (180 meV) barrier (TS3) to lose a hydrogen and form $C_3H_3^+$. This barrier is too high for the ∼10 meV translational energy to surmount; yet, the alternative is relaxation to $C_3H_4^+$ (INT3). As $C_3H_3^+$ is the most abundant product, it suggests that the lifetime of $C_3H_4^+$ is sufficiently long for the hydrogen to tunnel. This is consistent with the fact that the low pressure system ($\lesssim 10^{-9}$ Torr) significantly reduces the probability of energy quenching from background-gas collisions.

In addition to the Jahn−Teller distortion of allene, there are a few other distinctions between the C_3 H_4 isomers that may contribute to the differing reaction mechanism. The first factor is the exothermicity of both reactions. The acetylene−allene charge transfer is more exothermic than that of the acetylene-propyne. This would indicate that long-range charge exchange is kinetically preferred for allene over propyne by the generalized Mulliken−Hush treatment of electron transfer.[95] A second consideration is the dipole moments of propyne and allene. Larger dipole moments result in greater Langevin capture radii, which increase the likelihood of an association complex. While the dipole moment for propyne is small, allene does not have one. Consequently, this Langevin capture picture also suggests that propyne is more likely to form a bonded complex than allene. It should be noted that there is also a possibility that the allene and acetylene ion reactions may take place on an excited potential energy surface, which could influence the reaction mechanism as well. However, further exploration of this concept was beyond the scope of the original theoretical work.

In summary, we were able to determine contrasting reaction mechanisms for the reaction of the acetylene ion with two different isomers of C_3H_4. This was initially detected by studying the branching of the product with respect to reactant isotopologues, and further verified by theoretical potential energy surfaces. In the propyne case, a short-range charge transfer was followed by a reaction complex formation. This contrasted the case of acetylene ion and allene, where the product was either $C_3H_3^+$ or $C_3D_3^+$ and indicated long-range charge transfer and unimolecular isomerization. Our high-resolution TOF-MS was critical for identifying and quantifying neighboring mass channels and enabling this analysis to take place.

RADIOFREQUENCY TRAPPING AND CHEMISTRY WITH CCL^+

Methods for studying ion-neutral chemical reaction studies can, broadly speaking, be split into two categories: beam- or flow-based methods and trap-based methods. Each approach has advantages and trade-offs, but the concern of this section is the advantages of trapped ion studies. The primary advantages of working with trapped ions in ion-neutral chemical physics studies are the stability of the trap, the broad mass range of the trapping fields, and the ability for selective ejection (cleaning) of ions from the trap.

One advantage of working with ion-neutral studies on ion traps is the inherent stability of ion traps. Trapped ions in sufficiently deep RF potentials and under (very clean) UHV

https://doi.org/10.1021/acs.jpca.3c07546
J. Phys. Chem. A 2024, 128, 1737−1752

conditions can be trapped for days. As such, even very slow reactions can be observed without systematic losses of ions from the trap. In addition, when ions are loaded into the trap in excited electronic or vibrational states, it is technically trivial to wait and allow the system to relax to a distribution characteristic of the ambient temperature of the ion trap. This is true even for excited states with lifetimes on the order of seconds. This capability greatly simplifies the loading of ions from ionization schemes that can leave ions in excited states, which has historically complicated measurements in beams and flow tubes, where the timings from excitation to reaction are preset by the dimensions of the apparatus.

Another advantage of RF traps is the range of m/z ratios that can be trapped within an ion trap. The exact range depends on the number of poles in the trap, the depth of the trap, trap dimensions, and the frequency. As an example, for our RF frequency of 3.555 MHz, we can trap down to m/z 12 (but lower masses cannot be stably trapped), and up to $m/z \sim 300$ (where higher masses would have a trap depth less than 2 eV.) In practice, we have worked with m/z 17−136, ammonia to xenon. An important result of this large working range is not just the flexibility in the ions that can be loaded as reactants but also the ability to trap a large range of relevant products, even when the reaction is quite exothermic. This is important for identifying the products as well as the measurement of branching ratios. Since we detect the reaction products as well as the reactants, we can expect the total number of ions in our trap to remain constant. Observation of charge conservation in the trap lends credibility to any claims about product identity, order, and branching ratios.

Electrodynamic traps contribute some challenges and opportunities due to the heating of trapped ions. Linear quadrupole ion traps have micromotion heating of the ions that increases the further ions off the trap axis as the magnitude of the RF increases. For this reason, traps with more poles, especially 22-pole ion traps, are a favored alternative to quadrupole traps, as they contribute significantly less to micromotion heating due to the very flat potential (low RF magnitude) near the center of the trap. However, optical access is very limited and the confining potential is relatively weak.[34] Thus, quadrupole traps have the benefit of being more easily translationally cooled without the added complexity of techniques such as buffer gas cooling. Although ions in a quadrupole trap experience more micromotion heating, they have harmonic secular frequencies associated with their m/z, which can allow for selectively ejecting particular ions from the trap. This technique can be applied to produce a clean reactant sample before the start of a reaction. This can done by driving a dipolar excitation,[66] where the location of the trap center is oscillated at the secular frequency of the unwanted ion or a quadrupolar excitation,[67] in which the trap depth is modulated at the secular frequency. (Typical secular frequencies are on the order of ∼100 kHz in our ion trap.) In our experiment, we found quadrupolar excitations to be more effective at ejecting ions without ejecting nearby masses. This cleaning technique was also used in by Puri et al. in the reaction of $BaOCH_3^+ + Ca(^3P_J)$ in an atom-ion hybrid trap.[96]

It should be noted that the ability to clean an ion sample is not unique to ion traps. The same principle that allows cleaning from an ion trap forms the basis of filtration with quadrupole mass filters, a technique featured in reactions with ion beams and selected ion flow tube experiments.[25,97] Likewise, ion storage ring methods also allow for mass selection of reactant ions.[98] These experiments operate under somewhat different environmental conditions from Coulomb crystals (such as higher background pressure, larger collision energies, etc.) However, Coulomb crystals do uniquely pair this capability with the other described features of this apparatus. Since linear ion traps do allow this selectivity of ion reactants, it is a natural feature to utilize in Coulomb crystal studies.

Therefore, this technique has become a routine step in our ion loading process for all reaction studies but was critical for our investigations of the ion CCl^+. As will be discussed in the following section, this ion is interesting for astrochemistry but is difficult to isolate and study experimentally. In particular, we determined a laser ionization scheme to produce CCl^+ ion from a tetrachloroethylene (C_2Cl_4) precursor. This scheme uses nonresonant photoionization with UV light, which produces a variety of fragments: $^{35}Cl^+$, $^{37}Cl^+$, C_2^+, $C^{35}Cl^+$, $C^{37}Cl^+$, $C_2{}^{35}Cl^+$, $C_2{}^{37}Cl^+$, etc. An example mass spectrum before cleaning can be seen in Figure 9a. The effectiveness of

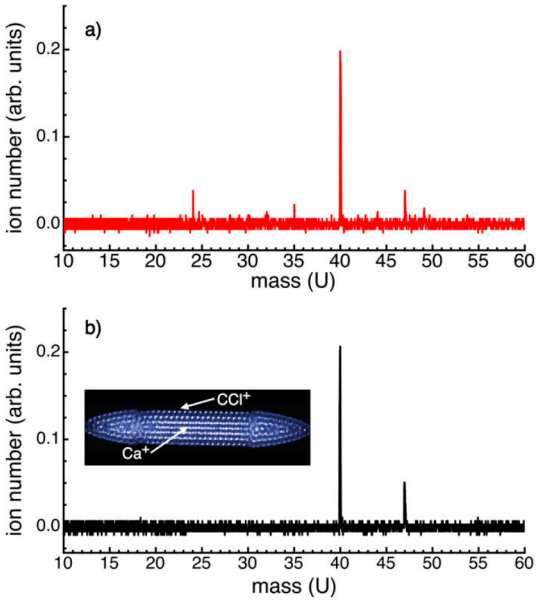

Figure 9. TOF traces for an ion trap (a) before and (b) after cleaning using RF excitations. After cleaning, only Ca^+ (m/z 40) and CCl^+ (m/z 47) remain in quantities greater than a few ions. Also included as an inset is a false-color CCD image of the ions, showing that the Coulomb crystal is deformed by the heavier CCl^+ ions that sit around the outside of Ca^+ in the radial direction. Reprinted from Krohn et al. *J. Chem. Phys.* **2021**, *154*, 074305[100] with the permission of AIP Publishing.

secular excitation cleaning can be observed from the example spectrum in Figure 9b. The high purity with which we prepare $C^{35}Cl^+$ or $C^{37}Cl^+$ in our trap allowed us to investigate CCl^+ by reacting it with three molecules: acetylene (C_2H_2),[99] acetonitrile (CH_3CN),[100] and benzene ($cC_6H_6^+$).[101] All three of these reactions demonstrated interesting and astrochemically relevant products that indicate the reactivity of CCl^+ with astrochemically relevant neutral molecules. These studies were only feasible due to the secular frequency cleaning technique that is enabled by the harmonic potential of the trap. The details of the CCl^+ reaction with acetonitrile will be discussed in the next section.

https://doi.org/10.1021/acs.jpca.3c07546
J. Phys. Chem. A 2024, 128, 1737−1752

The Isotope-Resolved Reaction of Acetonitrile with CCl^+. CCl^+ is of particular interest for astrochemical investigations as a potential reservoir for chlorine in space. However, it has been absent from ion-neutral gas-phase studies for all but a few select reactions. One major contribution to the scarcity of previous research on CCl^+ reactivity is the difficulty in isolating it in most experimental platforms. CCl^+ needs to be created by fragmentation from a precursor and, thus, requires significant filtering of the other fragments produced from its generation. Such filtering had not been feasible in most ion-neutral reaction experiments until now.

Nevertheless, many chlorine-containing compounds have been discovered in the ISM,[102−108] and, thus, understanding the reactivity of CCl^+ is important for understanding chlorine chemistry in space. CCl^+ itself has yet to be detected, although it is expected to be present and is usually included in theoretical models of ISM chemistry.[109−111] While CCl^+ has a demonstrated formation reaction from C^+ + HCl,[112] CCl^+ itself has only been reacted with a limited scope of astrochemically relevant molecules. A series of experiments demonstrated the reactivity of CCl^+ with NH_3, H_2CO, CH_3Cl, $CHCl_3$, CCl_4, $CHCl_2F$, and $CHClF_2$,[111,113−116] the first three of which are demonstrated to be in the ISM. However, CCl^+ was shown to be unreactive with NO, H_2, CH_4, N_2, O_2, CO, CO_2, HCN.[111,115,116] In the 30 years since these experiments, CCl^+ has been effectively overlooked in laboratory ion-neutral molecular reaction studies despite several gaps in our knowledge of its reactivity.

Our study of CCl^+ with acetonitrile (CH_3CN, CD_3CN) is the first experiment of an ion-neutral reaction between CCl^+ and a nitrile. We chose to react with a nitrile due to the importance of this group of molecules to astrochemistry. From smalls cyanides (HCN as well as DCN) found in the Orion Nebula decades ago[117,118] to the recent discovery of benzonitrile,[119] nitriles are well-established for their presence in the ISM and their notable role in prebiotic chemistry[120] and tholin formation[89] in planetary atmospheres. Acetonitrile has been detected in many regions of the cosmos, including the diffuse ISM,[121] cold and dark molecular clouds,[122] low mass protostars,[123−125] hot cores,[126−128] as well as several comets.[129−131] It is a critical astrochemical participant, and thus, its interactions with organohalogens are vital to understand.

This section will first provide an overview of the experimental results from mass spectrometry, demonstrating the information provided by clean selection of either chlorine isotope. Then, the energetics and potential energy surface are discussed, demonstrating how the theoretical calculations provide additional information on the reaction mechanism.

The CCl^+ + CH_3CN reaction showed two primary products (m/z 27 and m/z 62), which both reacted to a secondary product (m/z 42.) These products were identified as $C_2H_3^+$, $HNCCl^+$, and CH_3CNH^+, respectively. This was a nontrivial assignment, as there are multiple possibilities for these products. However, when comparing the mass shifts due to $C^{37}Cl^+$ and/or CD_3CN substitution, we were able to determine the number of hydrogen or chlorine atoms in each product, leaving these as the only possible chemical formulas for the products. The resulting normalized ion numbers plotted against the reaction time are shown in Figure 10. As can be seen from this plot, the solid lines that denote the pseudo-first-order rate reaction model fit the experimental data well. This, as well as the functional form of the growth in each mass

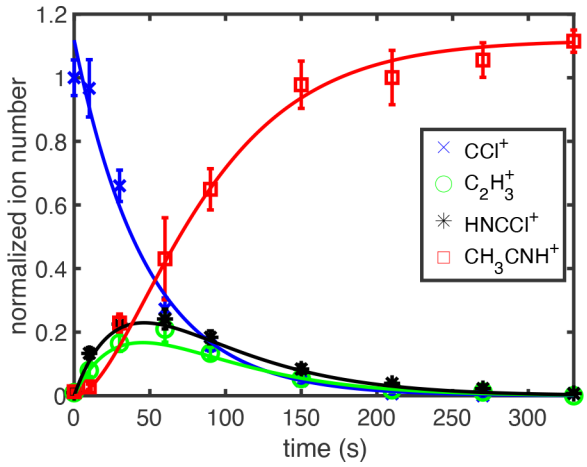

Figure 10. Normalized data from mass spectra demonstrating the change in ion trap masses as a function of exposure to CH_3CN. CCl^+ decay and primary products $C_2H_3^+$ and $HNCCl^+$ are formed. Both primary products react with a second CH_3CN to form CH_3CNH^+. Each point and error bar represent the mean and standard error for 10 repetitions at each time point. Solid lines represent the best fit of the pseudo-first-order reaction rate model. Reprinted from Krohn et al. *J. Chem. Phys.* **2021**, *154*, 074305[100] with the permission of AIP Publishing.

channel, supports the reaction model shown in Figure 11. This assigns the two primary product channels to $C_2H_3^+$ + NCCl

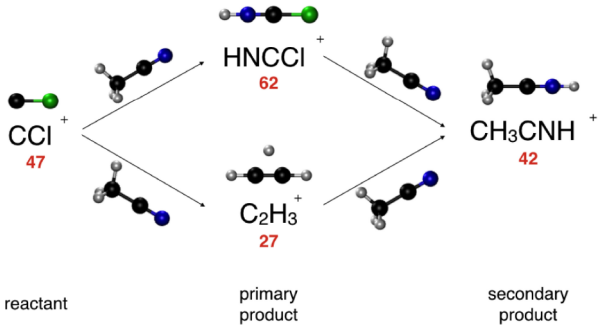

Figure 11. Diagram of the proposed reaction model for CCl^++ CH_3CN, identifying the reaction order and the identity of product ions. Each arrow indicates a reaction with a neutral CH_3CN molecule. Below the molecule, the numbers represent the measured m/z ratios for each product.

and $HNCCl^+$ + C_2H_2, with both ionic products reacting with a second acetonitrile to produce terminal products CH_3CNH^+ + C_2H_2/NCCl.

Identification and verification of these products also included a check of the exothermicity of all of the products. Both the primary products are exothermic, as can be seen from the potential energy surface shown in Figure 12. This potential energy surface was calculated at the [CCSD(T)/CBS//MP2/aug-cc-pVTZ] level of theory to investigate the dynamics and kinetics of the reaction. The surface includes four labeled products, as there are two different isomers possible for both $C_2H_3^+$ and C_2H_2.

As well as demonstrating a lack of barriers to the reaction, the PES provided insight into the reaction mechanism and kinetics. The first step of the reaction was determined to be INT1 regardless of the reactant approach direction. This is perhaps unsurprising, as chlorine has high electronegativity.

https://doi.org/10.1021/acs.jpca.3c07546
J. Phys. Chem. A 2024, 128, 1737−1752

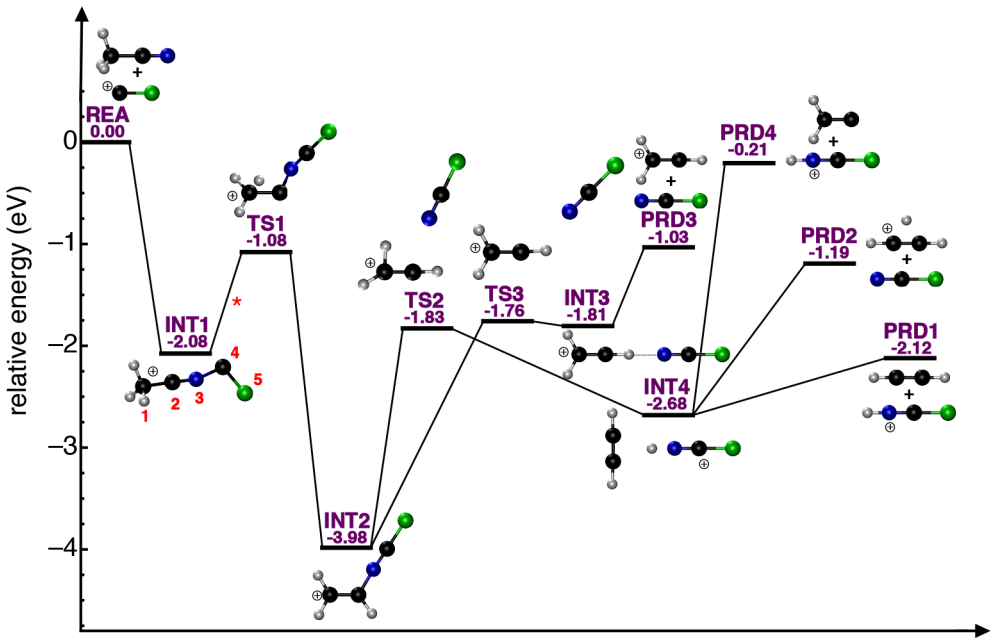

Figure 12. Potential energy surface for CCl^+ + CH_3CN, depicting stationary point geometries connecting the reactants (REA) to the products (PRD1, PRD2, PRD3, and PRD4). For these geometries, the bare "+" refers to infinite distance between the ion-neutral pair, while the "⊕" symbol indicates the ion of the ion-neutral pair. "INT" denotes intermediate states, while "TS" labels transition states. Geometries were calculated at the MP2/aug-cc-pVTZ level, with [CCSD(T)/CBS//MP2/aug-cc-pVTZ] energies. Reprinted from Krohn et al. *J. Chem. Phys.* **2021**, *154*, 074305[100] with the permission of AIP Publishing.

This results in a pull of electron density away from the C2−N3 triple bond and toward the chlorine group (See Figure 12 for labeling of atoms). After a hydrogen passes from C1 to C2 (TS1-INT2), the newly formed N3−C4 bond is shorter and stronger than the C2−N3. Ultimately, this originally strong C2−N3 triple bond is cleaved for all product pathways, and the nitrogen and chlorine atoms end up on the same molecule for all products. The surface splits from INT2 with the paths primarily differing in the behavior of the hydrogen atoms, as the C2−N3 bond stretches and eventually breaks. Four different product isomer combinations can be found. While we cannot distinguish between the two isomers of $C_2H_3^+$ (PRD2, PRD3) or C_2H_2 (PRD1, PRD4), we can measure the branching ratio of these two ionic products and compare them with Rice−Ramsperger−Kassel−Marcus (RRKM) and master equation (ME) theory calculations.

The kinetic behavior of this reaction was probed with statistical reaction rate theory calculations to compare with the experimental results. More details about the theoretical methods can be found in the original paper.[100] The reaction rates for $C_2H_3^+$ and $HNCCl^+$ for unsubstituted reactants were experimentally measured as 1.6(5) and 2.2(5) × $10^{-9}$$cm^3$/s, respectively (Table 2). This corresponds to a branching ratio of 43:56, which was well predicted by theory.[100] Note that this reaction is faster than the Langevin predictions at 1.11 × 10^{-9} cm^3/s. This likely results from the dipole moment and large dipole-locking constant (c) for acetonitrile, leading to a kinetic rate predicted by Average-Dipole-Orientation Theory (ADO) of 3.74 × 10^{-9} cm^3/s. This is in good agreement with the experimental measurement of 3.8(4) × 10^{-9} cm^3/s (Table 2). This suggests that for this reaction, there is very little reverse dissociation back into reactants; that is, capture nearly always leads to products.

The ability to compare the kinetics across different isotope substitutions also proved insightful. While theory only explored reactions with the abundant isotopologues, an interesting extension would be to compare calculated branching ratios with deuterium and/or ^{37}Cl. Experimentally, we see an interesting trend in the kinetic rates. As can be seen in Table 2, substitution with heavier isotopes appeared to correlate with higher reaction rate constants. A caveat must precede this discussion. Reaction rate constants are subject to systematic errors in the measurement of the neutral gas pressure. This is particularly true for UHV measurements with ion gauges. However, these systematic errors are more likely to affect absolute measurements of rate constants than comparisons across different isotopologues (CH_3CN, CD_3CN) of the same gas at similar pressures. For these reasons, the enhancement of the reaction rate by up to a factor of 1.6 may be noteworthy. This observed enhancement contrasts with expectations of ADO theory, which predicts small (<5%) reductions in rate constants with heavier isotopes. Inverse kinetic isotope effects are rather rare, but are suspected to play a role in deuterium fractionation in the ISM. While further work is required before a definite identification of an inverse KIE, this measurement is intriguing.

Table 2. Rate Constants for Isotopologue Variations of CCl^+ + CH_3CN Primary Products[a]

Reactants	$C_2X_3^+$	$XNCCl^+$	Total
CCl^+ + CH_3CN	1.6 ± 0.5	2.2 ± 0.5	3.8 ± 0.4
$C^{37}Cl^+$ + CH_3CN	2.9 ± 0.7	3.0 ± 0.7	5.9 ± 0.3
CCl^+ + CD_3CN	2.4 ± 0.5	3.0 ± 0.5	5.4 ± 0.3
$C^{37}Cl^+$ + CD_3CN	2.9 ± 0.8	3.4 ± 0.8	6.3 ± 0.3

[a]"X" represents a hydrogen or deuterium from acetonitrile. Rates are in units of ×10^{-9} cm^3/s, and the reported statistical uncertainty is the calculated 90% confidence interval. Reprinted from Krohn et al. *J. Chem. Phys.* **2021**, *154*, 074305[100] with the permission of AIP Publishing.

https://doi.org/10.1021/acs.jpca.3c07546
J. Phys. Chem. A 2024, 128, 1737−1752

In conclusion, we demonstrated the reaction of CCl^+ with an astrochemically relevant molecule. For the unsubstituted reactants, RRKM and ADO theory predicted the experimentally measured branching ratios and reaction rate constant, respectively. A preliminary indication of an inverse kinetic isotope effect was observed with the deuterated and ^{37}Cl-substituted reactants reacting faster. Not only does this reaction further indicate that CCl^+ could be quite reactive in the ISM, but it also demonstrated a notable mechanism driven by the electronegativity of the chlorine. The interaction of the organohalogen cation with the simple nitrile may suggest a trend relevant to reactions of CCl^+ and CF^+ with other nitriles in the ISM.

This reaction of $CCl^+ + CH_3CN$ was part of a larger effort of our group to measure reactions of CCl^+ with astrochemically relevant molecules. Features of our RF trap were employed to produce this ion with sufficient purity in two different isotopologues. This procedure significantly influenced the depth of information that was obtained from these endeavors. CCl^+ has not yet been seen in the ISM, but we hope that recent spectroscopic measurements by Asvany et al. will aid in the search for it.[132] In any case, the understanding of its potential for participation in reactions in the ISM and of its gas-phase chemical reactivity has improved in the past few years.

CONCLUSION

Studying ion-neutral reactions is an exciting pursuit, yielding insights into foundational chemical physics principles and providing clues for understanding the chemical evolution of the interstellar medium. There are many fruitful ways to study ion-neutral reactions, all of which yield certain benefits and drawbacks. In this work, we featured our LIT-TOFMS and surveyed its specific features, including control over quantum states, use of high-resolution time-of-flight mass spectrometry, and advantageous use of ion-specific heating in the trap. This has resulted in our demonstration of quantum-state-specific reactions, isomer-sensitive reaction mechanisms, and products and our exploration of the reactivity of an elusive and astrochemically relevant ion. Coulomb crystals provide an excellent environment for studies relevant to chemistry in space. Specifically, they allow ion-neutral studies to be conducted in a low-pressure environment without interruption from background gases. This environment provides a unique opportunity to investigate the chemistry that occurs in cold and diffuse environments in space. An example of a more specific challenge includes investigations of the chemistry of methanol cation (CH_3OH^+.) This ion is an abundant molecule of prebiotic interest in astrochemistry that is found in cold dark clouds.[133] Significant research has been devoted to understanding the formation of methanol as it relates to gas-phase chemistry and chemistry on the surface of dust grains and gas-phase chemistry.[134,135] Studies of CH_3OH^+ with astrochemically abundant molecules like NH_3, H_2, and H_2O in a Coulomb crystal environment may illuminate possible gas-phase interactions of the methanol cation after its formation.

There are exciting future directions for the field of ion-neutral chemistry in Coulomb crystals. One example is the construction or operation of cryogenic ion traps for studies of ion-neutral reactions.[136−138] Such an environment reduces the temperature of the neutral molecules as well as eliminates the excitation of ion rotational states by blackbody radiation by the chamber walls. A cryogenic ion trap thus reduces and allows for more control of the collision energy of chemical reactions in the ion trap. Such advancements will allow investigations of ion-neutral chemical dynamics at lower energies and conditions even more equivalent to the interstellar medium.

ASSOCIATED CONTENT

Data Availability Statement

The data that support the findings of this study are available in the Supporting Information and from the corresponding author upon reasonable request.

AUTHOR INFORMATION

Corresponding Author

H. J. Lewandowski − *JILA and the Department of Physics, University of Colorado, Boulder, Colorado 80309, United States;* orcid.org/0000-0002-0995-552X; Email: lewandoh@colorado.edu

Author

O. A. Krohn − *JILA and the Department of Physics, University of Colorado, Boulder, Colorado 80309, United States;* orcid.org/0000-0001-6214-0621

Complete contact information is available at: https://pubs.acs.org/10.1021/acs.jpca.3c07546

Notes

The authors declare no competing financial interest.

Biographies

Olivia A. Krohn received her Physics Ph. D. from the University of Colorado Boulder, within JILA. She worked with her advisor, Heather Lewandowski, to study translationally cold ion-neutral chemical reactions in a linear ion trap, utilizing techniques, such as ion-trapping, laser-cooling, time-of-flight mass spectrometry, and quantum chemical calculations. Her research interests concerned reactions of importance to chemical dynamics and astrochemistry. At the beginning of 2024, she became a postdoctoral appointee at the Combustion Research Facility (CRF) at Sandia National Labs and will become a Jill Hruby Postdoctoral Fellow within CRF in the fall. At CRF, her research interests are inelastic collisions in crossed molecular beams with highly resolved velocity, with velocity map ion imaging techniques.

Heather J. Lewandowski is a professor of physics and Fellow of JILA at the University of Colorado Boulder. She earned her B.S. degree in physics at Michigan Technological University in 1997 and her PhD in physics in 2002 at the University of Colorado working on Bose−Einstein condensation with Eric Cornell. Before joining the faculty at the University of Colorado, she was a National Research Council Postdoctoral Fellow at the National Institute of Standards and Technology with Jun Ye.

ACKNOWLEDGMENTS

This work was supported by the National Science Foundation (PHY-1734006, CHE-1900294) and the Air Force Office of Scientific Research (FA9550-16-1-0117).

ADDITIONAL NOTE

[1]As the velocity distribution of the trapped ions are not described by a Maxwell−Boltzmann distribution, the word "temperature" is not technically applicable. However, it is common in the field to indicate average energy in units E/k_b, where k_b is Boltzmann's constant.

REFERENCES

(1) Tielens, A. G. The molecular universe. *Rev. Mod. Phys.* **2013**, *85*, 1021−1081.
(2) Ziurys, L. M. Interstellar molecules and their prebiotic potential. *Handbook of Astrobiology* **2018**, *2*, 147−164.
(3) Puzzarini, C.; Barone, V. A never-ending story in the sky: The secrets of chemical evolution. *Physics of Life Reviews* **2020**, *32*, 59−94.
(4) McGuire, B. A. 2021 Census of Interstellar, Circumstellar, Extragalactic, Protoplanetary Disk, and Exoplanetary Molecules. *Astrophysical Journal Supplement Series* **2022**, *259*, 30.
(5) Wakelam, V. A kinetic database for astrochemistry (KIDA). *Astrophysical Journal, Supplement Series* **2012**, *199*, 21.
(6) Anicich, V. G. Evaluated Bimolecular Ion−Molecule Gas Phase Kinetics of Positive Ions for Use in Modeling Planetary Atmospheres, Cometary Comae, and Interstellar Clouds. *J. Phys. Chem. Ref. Data* **1993**, *22*, 1469−1569.
(7) Wakelam, V.; Herbst, E.; Selsis, F. The effect of uncertainties on chemical models of dark clouds. *Astron. Astrophys.* **2006**, *451*, 551−562.
(8) Wakelam, V.; Smith, I. W.; Herbst, E.; Troe, J.; Geppert, W.; Linnartz, H.; Öberg, K.; Roueff, E.; Agúndez, M.; Pernot, P. e. a.; et al. Reaction networks for interstellar chemical modelling: Improvements and challenges. *Space Science Reviews* **2010**, *156*, 13−72.
(9) Smith, I. W. Laboratory astrochemistry: Gas-phase processes. *Annual Review of Astronomy and Astrophysics* **2011**, *49*, 29−66.
(10) Snow, T. P.; Bierbaum, V. M. Ion chemistry in the interstellar medium. *Annual Review of Analytical Chemistry* **2008**, *1*, 229−259.
(11) Smith, D. The Ion Chemistry of Interstellar Clouds. *Chem. Rev.* **1992**, *92*, 1473−1485.
(12) Geppert, W. D.; Larsson, M. Experimental investigations into astrophysically relevant ionic reactions. *Chem. Rev.* **2013**, *113*, 8872−8905.
(13) Tsikritea, A.; Diprose, J. A.; Softley, T. P.; Heazlewood, B. R. Capture theory models: An overview of their development, experimental verification, and applications to ion−molecule reactions. *J. Chem. Phys.* **2022**, *157*, 60901.
(14) Langevin, P. M. Une formule fondamentale de theorie cinetique. *Annales de Chimie et de Physique, series* **1905**, *TS*, 245−288.
(15) Su, T.; Chesnavich, W. J. Parametrization of the ion-polar molecule collision rate constant by trajectory calculations. *J. Chem. Phys.* **1982**, *76*, 5183−5185.
(16) Su, T.; Bowers, M. T. Theory of ion-polar molecule collisions. Comparison with experimental charge transfer reactions of rare gas ions to geometric isomers of difluorobenzene and dichloroethylene. *J. Chem. Phys.* **1973**, *58*, 3027−3037.
(17) Clary, D. C. Calculations of rate constants for ion−molecule reactions using a combined capture and centrifugal sudden approximation. *Mol. Phys.* **1985**, *54*, 605−618.
(18) Troe, J. Statistical adiabatic channel model for ion−molecule capture processes. *J. Chem. Phys.* **1987**, *87*, 2773−2780.
(19) Krems, R. V. Cold controlled chemistry. *Phys. Chem. Chem. Phys.* **2008**, *10*, 4079−4092.
(20) Shapiro, M.; Brumer, P. *Principles of the Quantum Control of Molecular Processes*; Wiley-VCH, 2003.
(21) Toscano, J.; Lewandowski, H. J.; Heazlewood, B. R. Cold and controlled chemical reaction dynamics. *Phys. Chem. Chem. Phys.* **2020**, *22*, 9180−9194.
(22) Heazlewood, B. R.; Softley, T. P. Towards chemistry at absolute zero. *Nature Reviews Chemistry* **2021**, *5*, 125−140.
(23) Bell, M. T.; Softley, T. P. Ultracold molecules and ultracold chemistry. *Mol. Phys.* **2009**, *107*, 99−132.
(24) Böhme, D. K. Experimental studies of positive ion chemistry with flow-tube mass spectrometry: Birth, evolution, and achievements in the 20th century. *Int. J. Mass Spectrom.* **2000**, *200*, 97−136.
(25) Adams, N. G.; Smith, D. The selected ion flow tube (SIFT); A technique for studying ion-neutral reactions. *International Journal of Mass Spectrometry and Ion Physics* **1976**, *21*, 349−359.
(26) Ard, S. G.; Viggiano, A. A.; Shuman, N. S. Old School Techniques with Modern Capabilities: Kinetics Determination of Dynamical Information Such as Barriers, Multiple Entrance Channel Complexes, Product States, Spin Crossings, and Size Effects in Metallic Ion−Molecule Reactions. *J. Phys. Chem. A* **2021**, *125*, 3503−3527.
(27) Potapov, A.; Canosa, A.; Jiménez, E.; Rowe, B. Uniform Supersonic Chemical Reactors: 30 Years of Astrochemical History and Future Challenges. *Angewandte Chemie - International Edition* **2017**, *56*, 8618−8640.
(28) Rowe, B. R.; Marquette, J. B. CRESU studies of ion/molecule reactions. *International Journal of Mass Spectrometry and Ion Processes* **1987**, *80*, 239−254.
(29) Wester, R. Velocity map imaging of ion−molecule reactions. *Phys. Chem. Chem. Phys.* **2014**, *16*, 396−405.
(30) Carrascosa, E.; Meyer, J.; Wester, R. Imaging the dynamics of ion−molecule reactions. *Chem. Soc. Rev.* **2017**, *46*, 7498−7516.
(31) Allmendinger, P.; Deiglmayr, J.; Schullian, O.; Höveler, K.; Agner, J. A.; Schmutz, H.; Merkt, F. New Method to Study Ion−Molecule Reactions at Low Temperatures and Application to the Reaction. *ChemPhysChem* **2016**, *17*, 3596−3608.
(32) Zhelyazkova, V.; Martins, F. B.; Agner, J. A.; Schmutz, H.; Merkt, F. Ion−Molecule Reactions below 1 K: Strong Enhancement of the Reaction Rate of the Ion-Dipole Reaction $He^+ + CH_3F$. *Phys. Rev. Lett.* **2020**, *125*, 263401.
(33) Zhelyazkova, V.; Martins, F. B. V.; Schilling, S.; Merkt, F. Reaction of an Ion and a Free Radical near 0 K: $He^+ + NO \rightarrow He + N^+ + O$. *J. Phys. Chem. A* **2023**, *127*, 1458−1468.
(34) Gerlich, D. Experimental investigations of ion−molecule reactions relevant to interstellar chemistry. *Journal of the Chemical Society, Faraday Transactions* **1993**, *89*, 2199−2208.
(35) Wester, R. Radiofrequency multipole traps: Tools for spectroscopy and dynamics of cold molecular ions. *Journal of Physics B: Atomic, Molecular and Optical Physics* **2009**, *42*, 154001.
(36) Dunn, G. H. Ion-electron and ion-neutral collisions in ion traps. *Phys. Scr.* **1995**, *T59*, 249−255.
(37) Okada, K.; Wada, M.; Takayanagi, T.; Ohtani, S.; Schuessler, H. A. Characterization of ion Coulomb crystals in a linear paul trap. *Physical Review A - Atomic, Molecular, and Optical Physics* **2010**, *81*, 013420.
(38) Willitsch, S. Coulomb-crystallised molecular ions in traps: Methods, applications, prospects. *Int. Rev. Phys. Chem.* **2012**, *31*, 175−199.
(39) Heazlewood, B. R.; Softley, T. P. Low-Temperature Kinetics and Dynamics with Coulomb Crystals. *Annu. Rev. Phys. Chem.* **2015**, *66*, 475−495.
(40) Drewsen, M.; Jensen, I.; Lindballe, J.; Nissen, N.; Martinussen, R.; Mortensen, A.; Staanum, P.; Voigt, D. Ion Coulomb crystals: A tool for studying ion processes. *Int. J. Mass Spectrom.* **2003**, *229*, 83−91.
(41) Heazlewood, B. R. Cold ion chemistry within Coulomb crystals. *Mol. Phys.* **2019**, *117*, 1934.
(42) Heazlewood, B. R.; Lewandowski, H. J. Chemistry Using Coulomb Crystals. *Emerging Trends in Chemical Applications of Lasers* **2021**, *1398*, 389.
(43) Willitsch, S. In *Advances in Chemical Physics*; Rice, S. A., Dinner, A. R., Eds.; John Wiley & Sons, 2017; Vol. *162*; pp 307−340. DOI: 10.1002/9781119324560.ch5.
(44) Schmid, P. C.; Greenberg, J.; Miller, M. I.; Loeffler, K.; Lewandowski, H. J. An ion trap time-of-flight mass spectrometer with high mass resolution for cold trapped ion experiments. *Rev. Sci. Instrum.* **2017**, *88*, 123107.
(45) Drewsen, M. Ion Coulomb crystals and some applications. *AIP Conf. Proceedings* **2003**, *606*, 135−144, DOI: 10.1063/1.1454277.
(46) Staanum, P. F.; Højbjerre, K.; Wester, R.; Drewsen, M. Probing isotope effects in chemical reactions using single ions. *Phys. Rev. Lett.* **2008**, *100*, 243003.
(47) Petralia, L. S.; Tsikritea, A.; Loreau, J.; Softley, T. P.; Heazlewood, B. R. Strong inverse kinetic isotope effect observed in ammonia charge exchange reactions. *Nat. Commun.* **2020**, *11*, 173.

(48) Tsikritea, A.; Park, K.; Bertier, P.; Loreau, J.; Softley, T. P.; Heazlewood, B. R. Inverse kinetic isotope effects in the charge transfer reactions of ammonia with rare gas ions. *Chemical Science* **2021**, *12*, 10005−10013.
(49) Zhelyazkova, V.; Martins, F. B. V.; Agner, J. A.; Schmutz, H.; Merkt, F. Multipole-moment effects in ion−molecule reactions at low temperatures: part I − ion-dipole enhancement of the rate coefficients of the He+ + NH3 and He+ + ND3 reactions at collisional energies Ecoll/kB near 0 K. *Phys. Chem. Chem. Phys.* **2021**, *23*, 21606−21622.
(50) Millar, T.; Bennett, A.; Herbst, E. Deuterium fractionation in dense interstellar clouds. *Astrophysical Journal* **1989**, *340*, 906−920.
(51) Schmid, P. C.; Greenberg, J.; Nguyen, T. L.; Thorpe, J. H.; Catani, K. J.; Krohn, O. A.; Miller, M. I.; Stanton, J. F.; Lewandowski, H. J. Isomer-selected ion−molecule reactions of acetylene cations with propyne and allene. *Phys. Chem. Chem. Phys.* **2020**, *22*, 20303−20310.
(52) Greenberg, J.; Schmid, P. C.; Thorpe, J. H.; Nguyen, T. L.; Catani, K. J.; Krohn, O. A.; Miller, M. I.; Stanton, J. F.; Lewandowski, H. J. Using isotopologues to probe the potential energy surface of reactions of. *J. Chem. Phys.* **2021**, *154*, 124310.
(53) Yang, T.; Li, A.; Chen, G. K.; Yao, Q.; Suits, A. G.; Guo, H.; Hudson, E. R.; Campbell, W. C. Isomer-specific kinetics of the C^+ + H_2Oreaction at the temperature of interstellar clouds. *Science Advances* **2021**, *7*, abe4080.
(54) Chang, Y. P.; Długołęcki, K.; Küpper, J.; Rösch, D.; Wild, D.; Willitsch, S. Specific chemical reactivities of spatially separated 3-aminophenol conformers with cold Ca^+ions. *Science* **2013**, *342*, 98−101.
(55) Kilaj, A.; Wang, J.; Straňák, P.; Schwilk, M.; Rivero, U.; Xu, L.; von Lilienfeld, O. A.; Küpper, J.; Willitsch, S. Conformer-specific polar cycloaddition of dibromobutadiene with trapped propene ions. *Nat. Commun.* **2021**, *12*, 6047.
(56) Xu, L.; Toscano, J.; Willitsch, S. Trapping and sympathetic cooling of conformationally selected molecular ions. *arXiv* **2023**, No. 2308.03935.
(57) Gingell, A. D.; Bell, M. T.; Oldham, J. M.; Softley, T. P.; Harvey, J. N. Cold chemistry with electronically excited Ca^+Coulomb crystals. *J. Chem. Phys.* **2010**, *133*, 194302.
(58) Bell, M. T.; Gingell, A. D.; Oldham, J. M.; Softley, T. P.; Willitsch, S. Ion−molecule chemistry at very low temperatures: Cold chemical reactions between Coulomb-crystallized ions and velocity-selected neutral molecules. *Faraday Discuss.* **2009**, *142*, 73−91.
(59) Okada, K.; Suganuma, T.; Furukawa, T.; Takayanagi, T.; Wada, M.; Schuessler, H. A. Cold ion-polar-molecule reactions studied with a combined Stark-velocity-filter-ion-trap apparatus. *Physical Review A - Atomic, Molecular, and Optical Physics* **2013**, *87*, 043427.
(60) Okada, K.; Sakimoto, K.; Takada, Y.; Schuessler, H. A. A study of the translational temperature dependence of the reaction rate constant between $CH_3CN$and Ne^+at low temperatures. *J. Chem. Phys.* **2020**, *153*, 124305.
(61) Dörfler, A. D.; Eberle, P.; Koner, D.; Tomza, M.; Meuwly, M.; Willitsch, S. Long-range versus short-range effects in cold molecular ion-neutral collisions. *Nat. Commun.* **2019**, *10*, 5429.
(62) Puri, P.; Mills, M.; Simbotin, I.; Montgomery, J. A.; Côté, R.; Schneider, C.; Suits, A. G.; Hudson, E. R. Reaction blockading in a reaction between an excited atom and a charged molecule at low collision energy. *Nat. Chem.* **2019**, *11*, 615−621.
(63) Yang, T.; Li, A.; Chen, G. K.; Xie, C.; Suits, A. G.; Campbell, W. C.; Guo, H.; Hudson, E. R. Optical Control of Reactions between Water and Laser-Cooled Be^+Ions. *J. Phys. Chem. Lett.* **2018**, *9*, 3555−3560.
(64) Greenberg, J.; Schmid, P. C.; Miller, M.; Stanton, J. F.; Lewandowski, H. J. Quantum-state-controlled reactions between molecular radicals and ions. *Phys. Rev. A* **2018**, *98*, 32702.
(65) Schmid, P. C.; Miller, M. I.; Greenberg, J.; Nguyen, T. L.; Stanton, J. F.; Lewandowski, H. J. Quantum-state-specific reaction rate measurements for the photo-induced reaction $Ca^+ + O_2 \rightarrow CaO^+ + O$. *Mol. Phys.* **2019**, *117*, 3036.
(66) Roth, B.; Blythe, P.; Schiller, S. Motional resonance coupling in cold multispecies Coulomb crystals. *Physical Review A - Atomic, Molecular, and Optical Physics* **2007**, *75*, 023402.
(67) Schmidt, J.; Hönig, D.; Weckesser, P.; Thielemann, F.; Schaetz, T.; Karpa, L. Mass-selective removal of ions from Paul traps using parametric excitation. *Appl. Phys. B: Laser Opt.* **2020**, *126*, 176.
(68) Wineland, D. J.; Bollinger, J. J.; Itano, W. M. Laser-Fluorescence Mass Spectroscopy. *Phys. Rev. Lett.* **1983**, *50*, 628−631.
(69) Takashi Baba, T. B.; Izumi Waki, I. W. Cooling and Mass-Analysis of Molecules Using Laser-Cooled Atoms. *Jpn. J. Appl. Phys.* **1996**, *35*, L1134.
(70) Mølhave, K.; Drewsen, M. Formation of translationally cold $MgH^+$and MgD^+molecules in an ion trap. *Physical Review A - Atomic, Molecular, and Optical Physics* **2000**, *62*, 011401.
(71) Kimura, N.; Okada, K.; Takayanagi, T.; Wada, M.; Ohtani, S.; Schuessler, H. A. Sympathetic crystallization of CaH^+produced by a laser-induced reaction. *Physical Review A - Atomic, Molecular, and Optical Physics* **2011**, *83*, 033422.
(72) Okada, K.; Wada, M.; Boesten, L.; Nakamura, T.; Katayama, I.; Ohtani, S. Acceleration of the chemical reaction of trapped Ca^+ions with H_2Omolecules by laser excitation. *Journal of Physics B: Atomic, Molecular and Optical Physics* **2003**, *36*, 33−46.
(73) Kilaj, A.; Käser, S.; Wang, J.; Straňák, P.; Schwilk, M.; Xu, L.; von Lilienfeld, O. A.; Küpper, J.; Meuwly, M.; Willitsch, S. Conformational and state-specific effects in reactions of 2,3-dibromobutadiene with Coulomb-crystallized calcium ions. *Phys. Chem. Chem. Phys.* **2023**, *25*, 13933−13945.
(74) Ratschbacher, L.; Zipkes, C.; Sias, C.; Köhl, M. Controlling chemical reactions of a single particle. *Nat. Phys.* **2012**, *8*, 649−652.
(75) Sandford, S. A.; Nuevo, M.; Bera, P. P.; Lee, T. J. Prebiotic Astrochemistry and the Formation of Molecules of Astrobiological Interest in Interstellar Clouds and Protostellar Disks. *Chem. Rev.* **2020**, *120*, 4616−4659.
(76) Vuitton, V.; Yelle, R. V.; McEwan, M. J. Ion chemistry and N-containing molecules in Titan's upper atmosphere. *Icarus* **2007**, *191*, 722−742.
(77) Smith, I. W. Gas-phase reactions in the ISM: Rate coefficients, temperature dependences, and reaction products. *Proceedings of the International Astronomical Union* **2011**, *7*, 361−371.
(78) Tajti, A.; Szalay, P. G.; Császár, A. G.; Kállay, M.; Gauss, J.; Valeev, E. F.; Flowers, B. A.; Vázquez, J.; Stanton, J. F. HEAT: High accuracy extrapolated ab initio thermochemistry. *J. Chem. Phys.* **2004**, *121*, 11599−11613.
(79) Wolk, A. B.; Leavitt, C. M.; Garand, E.; Johnson, M. A. Cryogenic Ion Chemistry and Spectroscopy. *Acc. Chem. Res.* **2014**, *47*, 202−210.
(80) Dodson, L. G.; Zagorec-Marks, W.; Xu, S.; Smith, J. E. T.; Weber, J. M. Intrinsic photophysics of nitrophenolate ions studied by cryogenic ion spectroscopy. *Phys. Chem. Chem. Phys.* **2018**, *20*, 28535−28543.
(81) Johnson, C. J.; Shen, B. B.; Poad, B. L. J.; Continetti, R. E. Photoelectron-photofragment coincidence spectroscopy in a cryogenically cooled linear electrostatic ion beam trap. *Rev. Sci. Instrum.* **2011**, *82*, 105105.
(82) Willitsch, S.; Bell, M. T.; Gingell, A. D.; Softley, T. P. Chemical applications of laser- and sympathetically-cooled ions in ion traps. *Phys. Chem. Chem. Phys.* **2008**, *10*, 7200−7210.
(83) Meyer, K. A.; Pollum, L. L.; Petralia, L. S.; Tauschinsky, A.; Rennick, C. J.; Softley, T. P.; Heazlewood, B. R. Ejection of Coulomb Crystals from a Linear Paul Ion Trap for Ion−Molecule Reaction Studies. *J. Phys. Chem. A* **2015**, *119*, 12449−12456.
(84) Rösch, D.; Gao, H.; Kilaj, A.; Willitsch, S. Design and characterization of a linear quadrupole ion trap for high-resolution Coulomb-crystal time-of-flight mass spectrometry. *EPJ. Techniques and Instrumentation* **2016**, *3*, 4434−4446.
(85) Schowalter, S. J.; Chen, K.; Rellergert, W. G.; Sullivan, S. T.; Hudson, E. R. An integrated ion trap and time-of-flight mass spectrometer for chemical and photo- reaction dynamics studies. *Rev. Sci. Instrum.* **2012**, *83*, 043103.

https://doi.org/10.1021/acs.jpca.3c07546
J. Phys. Chem. A 2024, 128, 1737−1752

(86) Krohn, O. A.; Catani, K. J.; P. Sundar, S.; Greenberg, J.; da Silva, G.; Lewandowski, H. J. Reactions of Acetonitrile with Trapped, Translationally Cold Acetylene Cations. *J. Phys. Chem. A* **2023**, *127*, 5120−5128.
(87) Lacy, J. H.; Evans, N. J., II; Achtermann, J. M.; Bruce, D. E.; Arens, J. F.; Carr, J. S. Discovery of interstellar acetylene. *Astrophysical Journal* **1989**, *342*, L43.
(88) Mumma, M. J.; DiSanti, M. A.; Dello Russo, N.; Magee-Sauer, K.; Gibb, E.; Novak, R. Remote infrared observations of parent volatiles in comets: A window on the early solar system. *Adv. Space Res.* **2003**, *31*, 2563−2575.
(89) Waite, J. H.; Young, D. T.; Cravens, T. E.; Coates, A. J.; Crary, F. J.; Magee, B.; Westlake, J. The Process of Tholin Formation in Titan ' s Upper Atmosphere. *Science* **2007**, *316*, 870−875.
(90) Agúndez, M.; Cernicharo, J.; Goicoechea, J. R. Formation of simple organic molecules in inner T Tauri disks. *Astron. Astrophys.* **2008**, *483*, 831−837.
(91) Lahuis, F.; van Dishoeck, E. F. ISO-SWS spectroscopy of gas-phase C_2H_2 and HCN toward massive young stellar objects. *Astron. Astrophys.* **2000**, *355*, 699−712.
(92) Knight, J. S.; Freeman, C. G.; McEwan, M. J.; Anicich, V. G.; Huntress, W. T. A flow tube study of ion−molecule reactions of acetylene. *J. Phys. Chem.* **1987**, *91*, 3898−3902.
(93) Anicich, V. G.; Blake, G. A.; Kim, J. K.; McEwan, M. J.; Huntress, W. T. Ion−molecule reactions in unsaturated hydrocarbons: allene, propyne, diacetylene, and vinylacetylene. *J. Phys. Chem.* **1984**, *88*, 4608−4617.
(94) Nguyen, T. L.; Stanton, J. F. A Steady-State Approximation to the Two-Dimensional Master Equation for Chemical Kinetics Calculations. *J. Phys. Chem. A* **2015**, *119*, 7627−7636.
(95) Newton, M. D.; Cave, R. J. In *Molecular Electronics*; Ratner, M. A., Jortner, E. J., Jortner, J., Ratner, M., Eds.; 1996; p 73.
(96) Puri, P.; Mills, M.; Schneider, C.; Simbotin, I.; Montgomery, J. A.; Côté, R.; Suits, A. G.; Hudson, E. R. Synthesis of mixed hypermetallic oxide BaOCa+ from laser-cooled reagents in an atom-ion hybrid trap. *Science* **2017**, *357*, 1370−1375.
(97) Herman, Z.; Futrell, J. H. Dynamics of ion−molecule reactions from beam experiments: A historical survey. *Int. J. Mass Spectrom.* **2015**, *377*, 84−92.
(98) Jinno, S.; Takao, T.; Hanada, K.; Goto, M.; Okuno, K.; Tanuma, H.; Azuma, T.; Shiromaru, H. Storage and mass-selective control of ions in an electrostatic ion storage ring. *Nuclear Instruments and Methods in Physics Research Section A: Accelerators, Spectrometers, Detectors and Associated Equipment* **2007**, *572*, 568−579.
(99) Catani, K. J.; Greenberg, J.; Saarel, B. V.; Lewandowski, H. J. Reactions of translationally cold trapped $CCl^+$with acetylene (C_2H_2). *J. Chem. Phys.* **2020**, *152*, 234310.
(100) Krohn, O. A.; Catani, K. J.; Greenberg, J.; Sundar, S. P.; Da Silva, G.; Lewandowski, H. J. Isotope-specific reactions of acetonitrile (CH_3CN) with trapped, translationally cold CCl^+. *J. Chem. Phys.* **2021**, *154*, No. 074305.
(101) Krohn, O. A.; Catani, K. J.; Lewandowski, H. J. Formation of astrochemically relevant molecular ions: Reaction of translationally cold $CCl^+$with benzene in a linear ion trap. *Phys. Rev. A* **2022**, *105*, L020801.
(102) Cernicharo, J.; Guelin, M. Metals in IRC + 10216: detection of NaCl, AlCl, and KCl, and tentative detection of AlF. *Astron. & Astrophys.* **1987**, *183*, L10−L12.
(103) Neufeld, D. A.; et al. Herschel Observations of Interstellar Chloronium. II. Detections toward G29.96−0.02, W49N, W51, AND W3(OH), and Determinations of the Ortho-to-Para and $^{35}Cl/^{37}Cl$ Isotopic Ratios. *Astrophysical Journal* **2015**, *807*, 54.
(104) Goto, M.; Usuda, T.; Geballe, T. R.; Menten, K. M.; Indriolo, N.; Neufeld, D. A. Fundamental vibrational transitions of hydrogen chloride detected in CRL 2136. *A&A* **2013**, *558*, L5.
(105) Zmuidzinas, J.; Blake, G. A.; Carlstrom, J.; Keene, J.; Miller, D. HCl Absorption toward Sagittarius B2. *Astrophysical Journal* **1995**, *447*, L125.
(106) Lis, D. C.; et al. Herschel/HIFI discovery of interstellar chloronium (H_2Cl^+). *Astron. Astrophys.* **2010**, *521*, L9.
(107) De Luca, M.; Gupta, H.; Neufeld, D.; Gerin, M.; Teyssier, D.; Drouin, B. J.; Pearson, J. C.; Lis, D. C.; Monje, R.; Phillips, T. G. e. a.; et al. HERSCHEL /HIFI DISCOVERY OF HCL$^+$IN THE INTERSTELLAR MEDIUM. *Astrophysical Journal* **2012**, *751*, L37.
(108) Fayolle, E. C.; Öberg, K. I.; Jørgensen, J. K.; Altwegg, K.; Calcutt, H.; Müller, H. S.; Rubin, M.; van der Wiel, M. H.; Bjerkeli, P.; Bourke, T. L.; et al. Protostellar and cometary detections of organohalogens. *Nature Astronomy* **2017**, *1*, 703−708.
(109) Neufeld, D. A.; Wolfire, M. G. The chemistry of interstellar molecules containing the halogen elements. *Astrophys. J.* **2009**, *706*, 1594−1604.
(110) Neufeld, D. A.; Wiesemeyer, H.; Wolfire, M. J.; Jacob, A. M.; Buchbender, C.; Gerin, M.; Gupta, H.; Güsten, R.; Schilke, P. The Chemistry of Chlorine-bearing Species in the Diffuse Interstellar Medium, and New SOFIA/GREAT Observations of HCL$^+$. *Astrophysical Journal* **2021**, *917*, 104.
(111) Blake, G. A.; Anicich, V. G.; Huntress, W. T. Chemistry of chlorine in dense interstellar clouds. *Astrophys. J.* **1986**, *300*, 415−419.
(112) Glosik, J.; Smith, D.; Španěl, P.; Freysinger, W.; Lindinger, W. SIFDT studies of the reactions of C^+, CH^+ and CH_2^+ with HCl and CO_2, and with HCl. *International Journal of Mass Spectrometry and Ion Processes* **1993**, *129*, 131−143.
(113) McAskill, N. A. Ion−molecule reactions in Trihalo- and Tetrahalo-methanes. *Aust. J. Chem.* **1970**, *23*, 893−903.
(114) Herod, A.; Harrison, A.; McAskill, N. Ion−Molecule Reactions in Methyl Fluoride and Methyl Chloride. *Can. J. Chem.* **1971**, *49*, 2217−2222.
(115) Anicich, V. G. Evaluated Bimolecular Ion−Molecule Gas Phase Kinetics of Positive Ions for Use in Modeling Planetary Atmospheres, Cometary Comae, and Interstellar Clouds. *J. Phys. Chem. Ref. Data* **1993**, *22*, 1469−1569.
(116) Smith, D.; Adams, N. G. Production and loss process for HC1 in interstellar clouds: some relevant laboratory measurements. *Astrophy. J.* **1985**, *298*, 827−829.
(117) Snyder, L. E.; Buhl, D. Observations of Radio Emission from Interstellar Hydrogen Cyanide. *Astrophys. J. Lett.* **1971**, *163*, L47.
(118) Jefferts, K. B.; Penzias, A. A.; Wilson, R. W. Deuterium in the Orion Nebula. *Astrophys. J. Lett.* **1973**, *179*, L57.
(119) McGuire, B. A.; Burkhardt, A. M.; Kalenskii, S.; Shingledecker, C. N.; Remijan, A. J.; Herbst, E.; McCarthy, M. C. Detection of the aromatic molecule benzonitrile ($c - C_6H_5CN$) in the interstellar medium. *Science* **2018**, *359*, 202−205.
(120) Ali, A.; Sittler, E. C.; Chornay, D.; Rowe, B. R.; Puzzarini, C. Organic chemistry in Titan's upper atmosphere and its astrobiological consequences: I. Views towards Cassini plasma spectrometer (CAPS) and ion neutral mass spectrometer (INMS) experiments in space. *Planet. Space Sci.* **2015**, *109−110*, 46−63.
(121) Solomon, P. M.; Jefferts, K. B.; Penzias, A. A.; Wilson, R. W. Detection of Millimeter Emission Lines from Interstellar Methyl Cyanide. *Astrophys. J.* **1971**, *168*, L107.
(122) Matthews, H. E.; Sears, T. J. Detection of the $J = 1 \rightarrow 0$transition of CH_3CN. *Astrophys. J. Lett.* **1983**, *267*, L53−L57.
(123) Codella, C.; Benedettini, M.; Beltrán, M. T.; Gueth, F.; Viti, S.; Bachiller, R.; Tafalla, M.; Cabrit, S.; Fuente, A.; Lefloch, B. Methyl cyanide as tracer of bow shocks in L1157-B1. *Astron. Astrophys.* **2009**, *507*, L25−L28.
(124) Bisschop, S. E.; Jørgensen, J. K.; Bourke, T. L.; Bottinelli, S.; van Dishoeck, E. F. An interferometric study of the low-mass protostar IRAS 16293−2422: small scale organic chemistry. *Astron. Astrophys.* **2008**, *488*, 959−968.
(125) Belloche, A.; Müller, H. S. P.; Garrod, R. T.; Menten, K. M. Exploring molecular complexity with ALMA (EMoCA): Deuterated complex organic molecules in Sagittarius B2(N2). *Astron. Astrophys.* **2016**, *587*, A91.
(126) Cazaux, S.; Tielens, A. G. G. M.; Ceccarelli, C.; Castets, A.; Wakelam, V.; Caux, E.; Parise, B.; Teyssier, D. The Hot Core around

the Low-Mass Protostar IRAS 16293−2422: Scoundrels Rule! *Astrophys. J.* **2003**, *593*, L51−L55.
(127) Bisschop, S. E.; Jørgensen, J. K.; van Dishoeck, E. F.; de Wachter, E. B. M. Testing grain-surface chemistry in massive hot-core regions. *Astron. Astrophys.* **2007**, *465*, 913−929.
(128) Gerin, M.; Combes, F.; Wlodarczak, G.; Jacq, T.; Guelin, M.; Encrenaz, P.; Laurent, C. Interstellar detection of deuterated methyl cyanide. *Astron. Astrophys.* **1992**, *259*, L35−L38.
(129) Kissel, J.; Krueger, F. R. The organic component in dust from comet Halley as measured by the PUMA mass spectrometer on board Vega 1. *Nature* **1987**, *326*, 755−760.
(130) Biver, N.; Bockelée-Morvan, D.; Colom, P.; Crovisier, J.; Davies, J. K.; Dent, W. R. F.; Despois, D.; Gérard, E.; Lellouch, E.; Rauer, H. e. a.; et al. Evolution of the Outgassing of Comet Hale-Bopp (C/1995 O1) from Radio Observations. *Science* **1997**, *275*, 1915−1918.
(131) Morse, A. D.; Chan, Q. H. S. Observations of Cometary Organics: A Post Rosetta Review. *ACS Earth Space Chem.* **2019**, *3*, 1773−1791.
(132) Asvany, O.; Markus, C. R.; Nagamori, K.; Kohguchi, H.; Furuta, J.; Kobayashi, K.; Schlemmer, S.; Thorwirth, S. Pure Rotational Spectrum of CCl^+. *Astrophysical Journal* **2021**, *910*, 15.
(133) Catone, D.; Satta, M.; Castrovilli, M. C.; Bolognesi, P.; Avaldi, L.; Cartoni, A. Photoionization of methanol: a molecular source for the prebiotic chemistry. *Chem. Phys. Lett.* **2021**, *771*, 138467.
(134) Garrod, R.; Hee Park, I.; Caselli, P.; Herbst, E. Are gas-phase models of interstellar chemistry tenable? The case of methanol. *Faraday Discuss.* **2006**, *133*, 51−62.
(135) Cernicharo, J.; Marcelino, N.; Roueff, E.; Gerin, M.; Jimenez-Escobar, A.; Munoz Caro, G. M. Discovery of the Methoxy Radical, CH3O, toward B1: Dust Grain and Gas-Phase Chemistry in Cold Dark Clouds*. *Astrophysical Journal Letters* **2012**, *759*, L43.
(136) Miossec, C.; Hejduk, M.; Pandey, R.; Coughlan, N. J. A.; Heazlewood, B. R. Design and characterization of a cryogenic linear Paul ion trap for ion−neutral reaction studies. *Rev. Sci. Instrum.* **2022**, *93*, 33201.
(137) Schwarz, M.; Versolato, O. O.; Windberger, A.; Brunner, F. R.; Ballance, T.; Eberle, S. N.; Ullrich, J.; Schmidt, P. O.; Hansen, A. K.; Gingell, A. D. e. a.; et al. Cryogenic linear Paul trap for cold highly charged ion experiments. *Rev. Sci. Instrum.* **2012**, *83*, 83115.
(138) Okada, K.; Suganuma, T.; Furukawa, T.; Takayanagi, T.; Wada, M.; Schuessler, H. A. Cold ion-polar-molecule reactions studied with a combined Stark-velocity-filter-ion-trap apparatus. *Physical Review A - Atomic, Molecular, and Optical Physics* **2013**, *87*, 043427.

https://doi.org/10.1021/acs.jpca.3c07546
J. Phys. Chem. A 2024, 128, 1737−1752